ANNE FEENSTRA*

MINERALOGISCH–PETROGRAPHISCHES INSTITUT, UNIVERSITY OF BERNE, BALTZERSTRASSE 1, CH-3012 BERNE, SWITZERLAND

An EMP and TEM–AEM Study of Margarite, Muscovite and Paragonite in Polymetamorphic Metabauxites of Naxos (Cyclades, Greece) and the Implications of Fine-scale Mica Interlayering and Multiple Mica Generations

Coexisting white micas and plagioclase were studied by electron microprobe (EMP), and transmission and analytical electron microscopy (TEM–AEM) in greenschist- to amphibolite-grade metabauxites from Naxos. The TEM–AEM studies indicate that sub-micron scale $(0\cdot01–1\cdot0\ \mu m$ thick) semi-coherent intergrowths of margarite, paragonite and muscovite are common up to lower amphibolite conditions. If unrecognized, such small-scale mica interlayering can easily lead to incorrect interpretation of EMP data. Muscovite and paragonite in M_2 greenschist-grade Naxos rocks are mainly relics of an earlier high-pressure metamorphism (M_1). Owing to the medium-pressure M_2 event, margarite occurs in middle greenschist-grade metabauxites and gradually is replaced by plagioclase + corundum in amphibolite-grade metabauxites. The margarite displays minor $^{IV}Al_3{}^{VI}(Fe^{3+},Al)Si_{-3}{}^{VI}\square_{-1}$ and considerable $(Na,K)SiCa_{-1}Al_{-1}$ substitution, resulting in up to 44 mol % paragonite and 6 mol % muscovite in solution. The compositional variation of muscovite is mainly described by $^{VI}(Fe^{2+},Mg)Si^{VI}Al_{-1}{}^{IV}Al_{-1}$ and $^{VI}(Fe^{3+}Al_{-1})$ exchanges, the latter becoming dominant at amphibolite grade. Muscovite is significantly richer in Fe than margarite or paragonite. Ca–Na–K partitioning data indicate that margarite commonly has a significantly higher $Na/(Na+K+Ca)$ value than coexisting muscovite or plagioclase. Exceptions are found in several greenschist-grade rocks, in which M_1-formed muscovite may have failed to equilibrate with M_2 margarite. The sluggishness of K-rich micas to recrystallize and adjust compositionally to changing P–T conditions is also reflected in the results of mus-covite–paragonite solvus thermometry. Chemical data for Ca–Na micas from this study and literature data indicate that naturally coexisting margarite–paragonite pairs display considerably less mutual solubility than suggested by experimental work. The variable and irregular Na partitioning between margarite and muscovite as observed in many metamorphic rocks could largely be related to opposing effects of pressure on Na solubility in margarite and paragonite and/or non-equilibrium between micas.

KEY WORDS: Ca–Na–K mica; margarite; metabauxite; Naxos; sub-micron-scale mica interlayering

INTRODUCTION

Since 1970, many new occurrences of the brittle mica margarite, $Ca_2Al_2(Al_2Si_2)O_{10}(OH)_2$, have been reported from localities throughout the world. Most are in metamorphosed marls and calcic pelites but margarite is also found in metamorphosed basites, anorthosites, impure marbles and bauxites [see reviews by Frey et al. (1982) and Guidotti (1984)]. Till now relatively little attention has been given to the classical occurrence of margarite in emery rocks (Smith, 1850, 1851), where the mineral coexists with corundum and Fe(–Ti)-oxides.

From the literature, two main occurrences of margarite can be distinguished (see Frey et al., 1982;

Guidotti, 1984). The first type involves margarite as a prograde rock-forming mineral in lower greenschist to amphibolite facies rocks, either as a matrix mineral, or at higher grades, sometimes with a porphyroblastic habit. Best documented is the regional distribution and petrologic significance of prograde margarite in metamarls and calcic metapelites from the Swiss and Austrian Alps (e.g. Ackermand & Morteani, 1973; Höck, 1974; Frey & Orville, 1974; Frey, 1978; Hoinkes, 1978; Frey et al., 1982; Frank, 1983; Bucher et al., 1983). Prograde margarite occurrences have also been reported from several other parts of the world, e.g. from France (Sagon, 1967), Norway (Andreasson & Lagerblad, 1980), NE Japan (Okuyama-Kusunose, 1985) and the Rocky Mountains in Canada (Gal & Ghent, 1991).

The second type, which has received much attention in the literature, involves margarite occurring as a pseudomorphic replacement of Al-rich minerals. Margaritization of andalusite and kyanite porphyroblasts is fairly common (e.g. Guidotti & Cheney, 1976; Guidotti et al., 1979; Cooper, 1980; Enami, 1980; Baltatzis & Katagas, 1981; Morand, 1988), but cases of replacement of sillimanite, corundum, chloritoid, staurolite, plagioclase, (clino)-zoisite and muscovite by margarite have also been described (e.g. Gibson, 1979; Teale, 1979; Frey et al., 1982; Yardley & Baltatzis, 1985; Grew et al., 1986; Stähle et al., 1986). Textural evidence commonly suggests that such margarite is not a peak metamorphic mineral but developed during the waning (retrograde) stages of the metamorphic cycle, and/or during polymetamorphism. The margarite probably largely formed by means of local ion-exchange reactions between the Al-rich precursor and Ca-rich fluids. The fact that Al-silicates, chloritoid and staurolite have high Al/Si ratios similar to those of margarite may facilitate margaritization of these minerals.

In rocks high in Al and Ca, margarite thus forms over a wide range of physico-chemical conditions, during progressive regional metamorphism as well as retrogressive and polymetamorphic events. Problems can thus arise regarding the petrogenetic significance of margarite in cases where it is unclear from textural and chemical evidence at which stage of the P–T–t history of a rock the mineral formed.

On Naxos, prograde margarite is an important constituent of emery deposits ranging in metamorphic grade from middle greenschist ($\sim 450°C$) to middle amphibolite facies ($\sim 620°C$). This paper deals with the mineralogical aspects of margarite and associated muscovite, paragonite and plagioclase in the Naxos metabauxites, discusses the Ca–Na–K partitioning among these minerals, and also addresses the problems involved with electron microprobe analysis of white micas interlayered on a submicron scale. The final part of the paper focuses on the somewhat puzzling phase relations among the Ca-, Na- and K-micas and discusses the complications of fine-scale mica interlayering and multiple mica generations in polymetamorphic rocks. A second paper (A. Feenstra, in preparation) will deal with the complete petrologic phase relations in calcic metabauxites, including a model for the progressive regional metamorphism of such Al-excess rocks.

GEOLOGICAL SETTING AND METAMORPHIC PETROLOGY

The island of Naxos is part of the Attic–Cycladic Metamorphic Complex (ACMC), which stretches from mainland Greece to SW Turkey (Fig. 1). The ACMC is essentially a nappe pile of predominantly Mesozoic sedimentary and volcanic rocks metamorphosed at various conditions. Petrologic and geochronologic studies (e.g. Andriessen et al., 1979; Van der Maar & Jansen, 1983; Feenstra, 1985; Dürr, 1986; Wybrans & McDougall, 1986, 1988; Dixon et al., 1987; Schliestedt et al., 1987; Okrusch & Bröcker, 1990) indicate that the ACMC rocks have experienced two main Alpine metamorphisms; an early Alpine high-pressure phase, M_1, which ended at 40–50 Ma and a medium-pressure Barrovian-type phase at 20–25 Ma (see Fig. 1). On virtually all Cycladic islands, the Eocene M_1 phase is expressed by blueschist facies mineralogies (locally with eclogite-facies assemblages), which are in varying degrees overprinted by the M_2 event. The high-P mineral assemblages formed during the collision of microplates with the Eurasian continent (e.g. Robertson & Dixon, 1984; Dürr, 1986; Jacobshagen, 1994). During the M_2 event, greenschist-grade rocks were formed on most islands, but metamorphic conditions locally reached upper amphibolite grade with associated migmatitization (e.g. on Naxos and Paros). Pre-Alpine basement is locally exposed as the lowest tectonic unit in windows on Ios, Sikinos and Naxos (see Fig. 1). The basement consists of (leuco)gneisses affected by Hercynian (~ 300 Ma) medium-pressure metamorphism and pre-Hercynian intrusive rocks (Van der Maar et al., 1981; Van der Maar & Jansen, 1983; Andriessen et al., 1987).

Isoclinally folded sequences of metasediments (pelitic and psammitic schists and gneisses, quartzites, calcitic and dolomitic marbles) and metavolcanics (amphibolites, basic schists) are the dominant lithologies of the ACMC. Metacarbonate units are widespread and contain in certain stratigraphic horizons metabauxite lenses (up to ~ 8 m
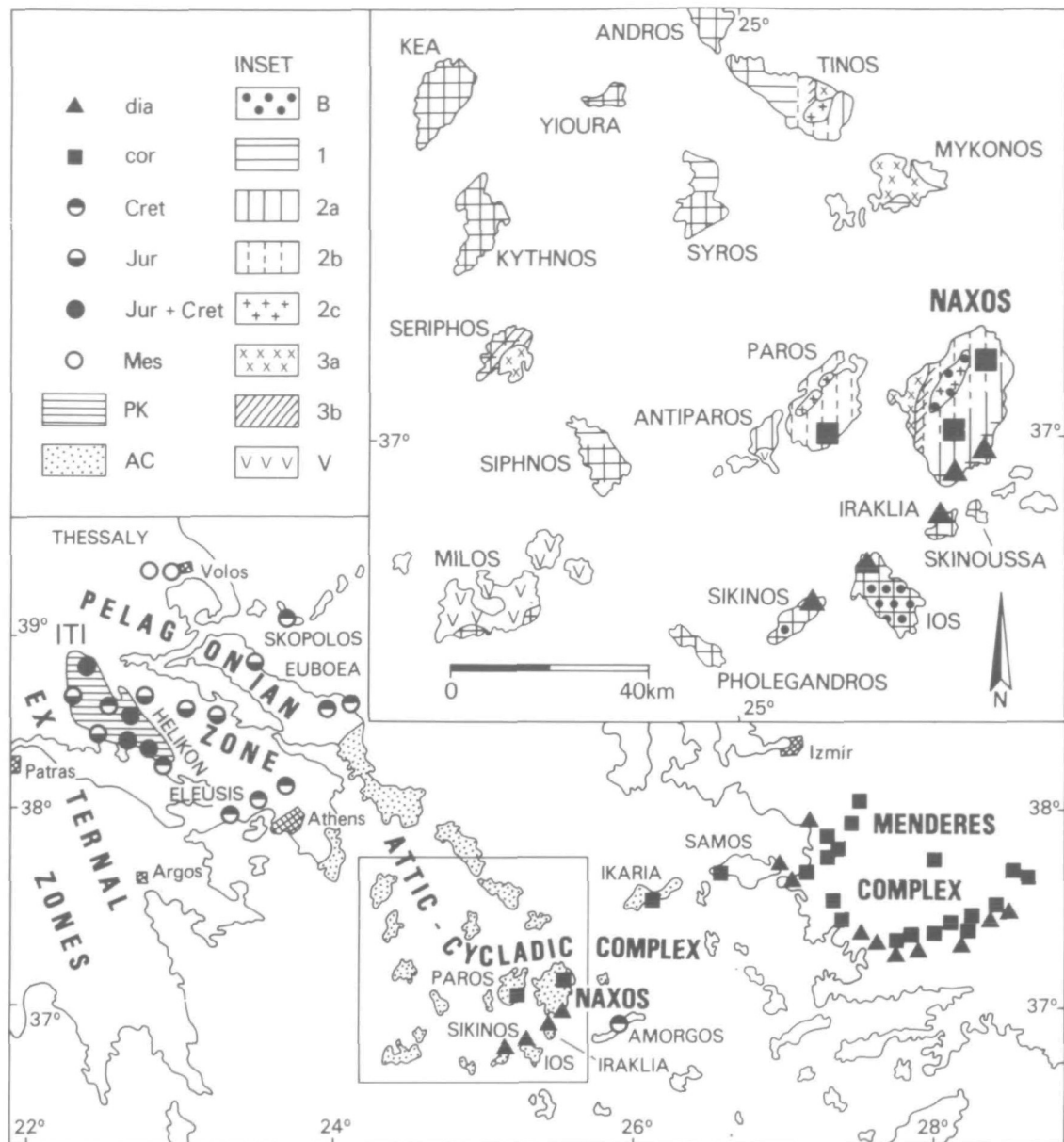
Fig. 1. Metamorphic map of the Cyclades and distribution of metabauxites and karstbauxites in the Aegean region (Feenstra, 1985). dia, diaspore-bearing metabauxites; cor, corundum-bearing metabauxites; Cret, Cretaceous karstbauxites; Jur, Jurassic karstbauxites; Jur + Cret, Jurassic and Cretaceous karstbauxites; Mes, Mesozoic karstbauxites of which the exact age is unknown; PK, Parnassos–Kiona zone; AC, Attic–Cycladic Metamorphic Complex; B, pre-Alpine basement; 1, M_1 glaucophane schist facies metamorphism; 2a, M_2 greenschist facies metamorphism; 2b, M_2 amphibolite facies metamorphism; 2c, M_2 migmatite; 3a, M3 granodiorite; 3b, M_3 contact metamorphism; V, Pliocene volcanism.

thick), which are of karstic origin. The metabauxites are diaspore-bearing (diasporites) on Sikinos, Ios, Iraklia and SE Naxos, and corundum-bearing (emeries) on most of Naxos and Paros (Fig. 1). Detailed petrological studies of the Cycladic metabauxites (Feenstra, 1985) indicate that they followed a $P–T–t$ path confined to the stability field of diaspore during M_1 and that dehydration into emery on Naxos and Paros occurred during the M_2 event.

Feenstra & Maksimovic (1985) inferred a Jurassic stratigraphic age for the Cycladic metabauxites from geochemical comparison with Mesozoic karstbauxites in Central Greece (Fig. 1).

The metamorphic complex of Naxos consists of a pre-Alpine high-grade migmatic gneiss and intrusive rock core, structurally covered by alternating series of marbles, schists and gneisses (Fig. 2). A discontinuous horizon of ultrabasic lenses enveloping
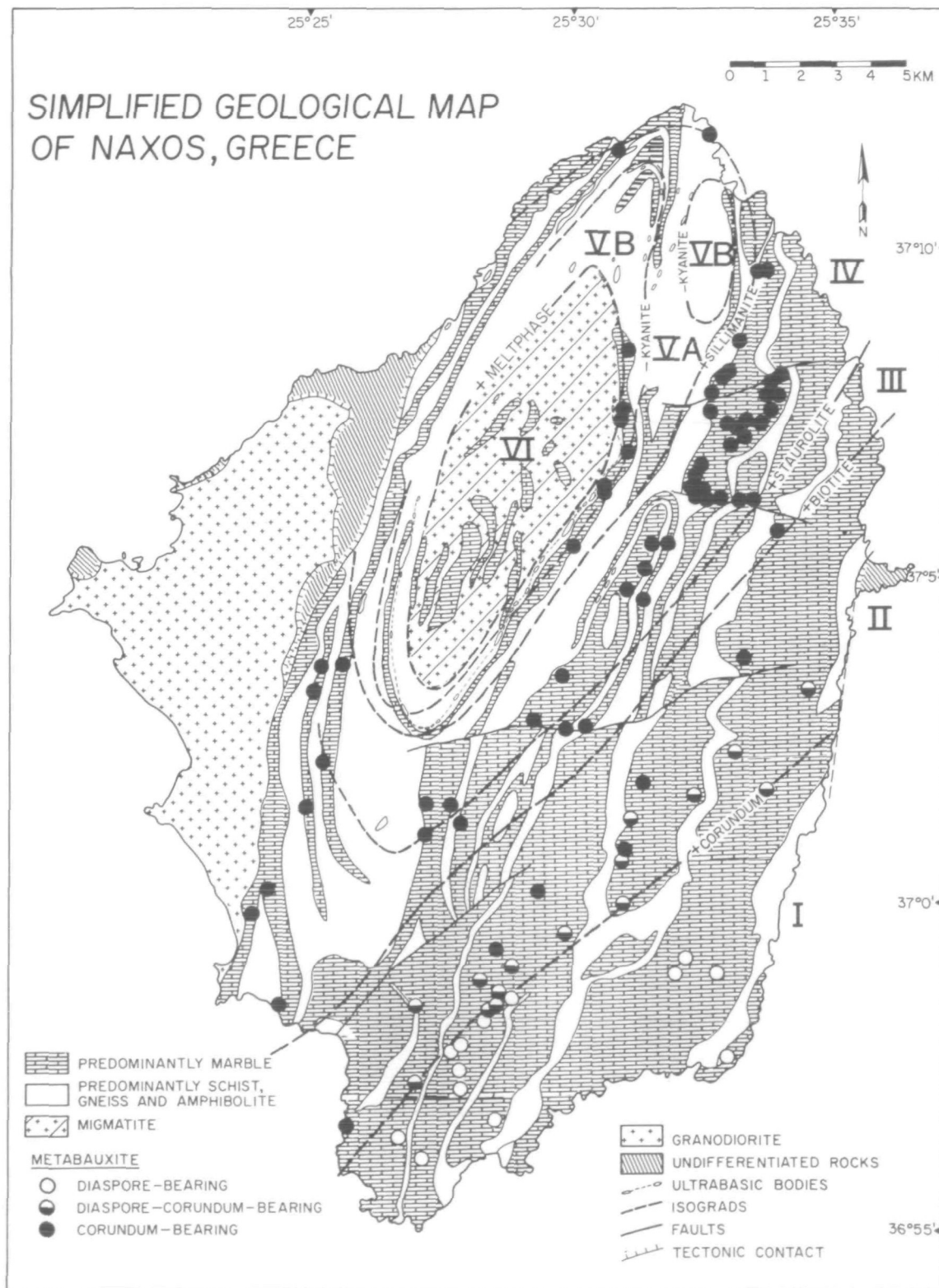
Fig. 2. Geological–petrological map of Naxos showing the distribution of metabauxite deposits, isograds and metamorphic zones I–VI (Feenstra, 1985).The following isograds were mapped with increasing M_2 grade: corundum-in (metabauxites); biotite-in (metapelites); Fe-rich staurolite-in (metabauxites and metapelites); sillimanite-in (metapelites); kyanite-out (metapelites); meltphase-in (metapelites). Estimated isograd temperatures are given in Fig. 3.

the NNE–SSW elongated migmatite dome-like core has been interpreted as marking the thrust plane along which the metamorphic complex was emplaced on top of the pre-Alpine basement (Van der Maar & Jansen, 1983; Andriessen *et al.*, 1987). During the M_2 event, the pre-Alpine rocks were remobilized at upper amphibolite-grade conditions and partially (re)melted. In the western part of Naxos an ~13 Ma old granodiorite intruded the metamorphic complex and induced andalusite–sillimanite type contact metamorphism in a zone of ~1 km width. In West Naxos a post-intrusive upper unit, comprising Tertiary sediments and ophiolite-suite rocks, tectonically overlies the metamorphic complex and granodiorite.

The metamorphic pattern of Naxos was shaped during the M_2 event, which culminated 15–20 Ma ago (Wybrans & McDougall, 1988). The pattern is defined by concentric zones of decreasing metamorphic grade outward from the high-grade migmatic core. Temperatures during the peak of M_2 ranged from ~700°C in the migmatite dome to ~400°C in SE Naxos at pressures of 5–7 kbar (Jansen & Schuiling, 1976; Jansen, 1977; Feenstra, 1985; Buick & Holland, 1989, 1991). Six isograds were mapped in metapelitic and metabauxitic rocks, which divide the complex into seven Barrovian-type metamorphic zones (see Figs 2 and 3).

The first appearance of corundum in the metabauxites has been mapped as the corundum-in isograd (T~420°C). The isograd separates diasporites characterized by the assemblage diaspore–chloritoid–muscovite–paragonite–calcite–haematite–rutile (zone I) from emeries containing the typical assemblage corundum–chloritoid–muscovite–paragonite–margarite–(Ti)haematite–rutile (zones II and III). Kyanite locally occurs in the metabauxites of zones I–III, particularly in Si-rich and Fe-poor deposits. In some diasporites from South Naxos, kyanite is associated with pyrophyllite and diaspore. Textural evidence suggests that the metabauxitic kyanite formed by the reaction

$$\text{pyrophyllite} + \text{diaspore} = \text{kyanite} + H_2O.$$
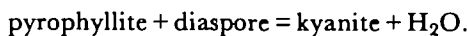
In contrast, kyanite in metapelitic rocks first appears in zone IV, more or less concomitant with the first appearance of staurolite (Jansen & Schuiling, 1976: A. Feenstra, unpublished data).

The first appearance of biotite in pelitic rocks, forming at the expense of chlorite and muscovite, defines the biotite-in isograd at T~500°C (Jansen & Schuiling, 1976). In the metabauxites, biotite is first found in zone IV (Fig. 3). Its formation is related to complex breakdown reactions of chloritoid and coincides with the income of staurolite
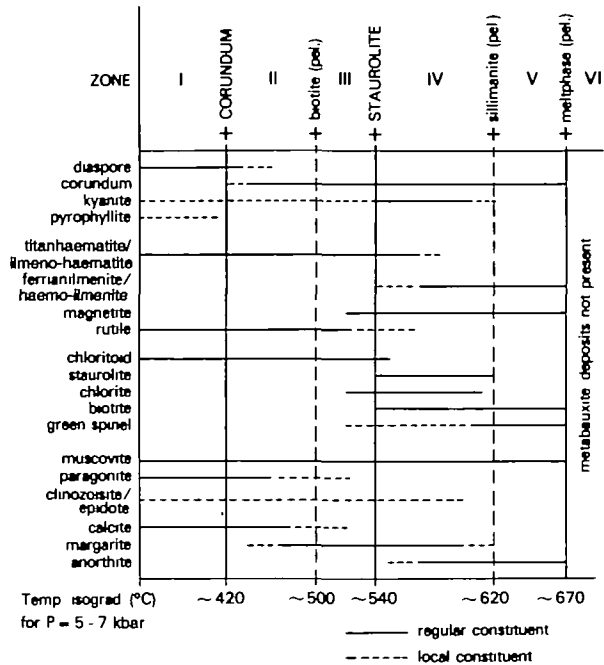

Fig. 3. Mineralogy of the metabauxites throughout the metamorphic zones of Naxos (Feenstra, 1985). The diagram only depicts primary mineral occurrences. Metamorphic zones and isograds are shown in Fig. 2.

(Feenstra, 1985, pp. 52–56). The first Fe-rich staurolite occurs at about similar metamorphic grade in bauxitic and pelitic rocks, marking the beginning of zone IV (T~540°C). Whereas some metabauxites contain coexisting chloritoid and staurolite (Feenstra, 1985), this assemblage is not known from the pelitic rocks.

The sillimanite-in, kyanite-out and meltphase-in isograds shown in Fig. 2 were mapped in metapelitic rocks by Jansen & Schuiling (1976). Pelitic schists of zone VA display pseudomorphic replacement of kyanite by sillimanite, providing support that part of the sillimanite grew directly from kyanite (Jansen & Schuiling, 1976; Jansen, 1977). More recent investigations of the high-grade portion of the metamorphic complex (Buick & Holland, 1989, 1991; Buick, 1991) showed that some fibrolitic sillimanite already occurs on the low-T side of the sillimanite-in isograd defined by Jansen & Schuiling (1976) and that some kyanite still persists in unmelted metapelite rafts embedded in sillimanite-bearing anatextic leucogneisses of zone VI.

Careful microscopic examination, and X-ray and electron microprobe studies have failed to detect any Al-silicate in the highest-grade emeries of zone VB, which are located slightly below the melt-in isograd (Fig. 2). Al-silicates formed at peak M_2 conditions may have been converted completely to retrograde

minerals during post-peak M_2 hydration and accompanying Ca-metasomatism that has generally affected these rocks (Feenstra, 1985). All emeries in zone VB are crosscut by networks of veinlets filled with retrograde minerals such as coarse margarite, Fe-rich chlorite and clinozoisite. Plagioclase is strongly altered to margarite and clinozoisite, biotite to chlorite, and staurolite to Fe-rich chlorite and gahnitic spinel. The retrogression has continued to low temperatures, as suggested by the presence of abundant diaspore and minor kaolinite. Comparable retrogradation as a result of the infiltration of water-rich fluids was documented in the marbles of the highest-grade areas of Naxos (Buick & Holland, 1991; Baker & Mathews, 1994). The hydrous fluids responsible for post-peak M_2 vein formation may have been derived from crystallizing melts at deeper levels when the metamorphic complex cooled during extensional uplift (Baker & Matthews, 1994).

The effect of the early Alpine (M_1) high-P metamorphism is pronounced in zones I and II. Metavolcanic lithologies in SE Naxos contain the assemblage quartz–glaucophane–epidote–phengite $\pm$ paragonite $\pm$ garnet, whereas metapelites contain the assemblage quartz–albite–chlorite–phengite $\pm$ paragonite $\pm$ garnet $\pm$ chloritoid (Jansen & Schuiling, 1976; Andriessen, 1978). Evidence of the M_1 event is also preserved in the pelitic rocks of zones III and IV, which still locally contain M_1 phengite (Si = 6·7–7·0 atoms per 22 O) that can texturally and chemically be distinguished from newly formed M_2 muscovite (Andriessen, 1978; Andriessen et al., 1979; Wybrans & McDougall, 1986, 1988; A. Feenstra, unpublished data). Isotopic age dating of white micas in pelitic and metabasic schists resulted up to staurolite grade in mixed ages of M_1 and M_2 (Andriessen et al., 1979; Wybrans & McDougall, 1986, 1988).

Up to the middle of zone IV metabauxites contain relict M_1 minerals such as muscovite, chloritoid, kyanite and clinozoisite–epidote, which have only partially reacted during M_2 (Feenstra, 1985). Because of its relict character and the scarcity of assemblages suitable for geothermobarometry, the P–T conditions during M_1 are poorly constrained on Naxos. Mineral assemblages in the SE Naxos rocks point to temperatures of ~400°C at pressures of ~9 kbar (Feenstra, 1985, and in preparation).

Whereas the early Alpine (pre- and syn-M_1) geological history of Naxos involved compressional tectonics related to crustal thickening and subduction of continental margin material, the late Alpine (syn- and post-M_2) tectonic evolution of the island involved rapid exhumation of the metamorphic rocks during crustal extension (Lister et al., 1984; Feenstra,
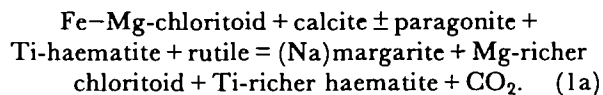
1985; Wybrans & McDougall, 1988; Urai et al., 1990; Buick, 1991).
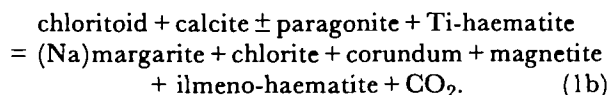
PETROLOGY OF THE METABAUXITES

Metabauxite deposits are locally enclosed in the Naxos marbles in all metamorphic zones, with the exception of the migmatite zone VI (Fig. 2). Most metabauxite lenses are part of discontinuous stratigraphic horizons. A detailed description of the geology, petrology and mineralogy of the Naxos metabauxites was given by Feenstra (1985). Figure 3 summarizes the metabauxitic mineralogy throughout the various metamorphic zones.

The metabauxites are very heterogeneous rocks, showing compositional variations on a millimetre to decimetre scale. The heterogeneity was largely inherited from the premetamorphic stage and reflects pisoidic textures, compositional banding, and other textural and geochemical characteristics of non-metamorphosed karst bauxites (Bardossy, 1982; Feenstra, 1985). The modal amount of white mica, therefore, varies from traces in the Al-rich commercial metabauxite up to 30–40% in the Si-rich, kyanite-bearing, type. Particularly in the commercial metabauxite, the white mica is irregularly distributed and concentrated in domains, completely surrounded by a corundum/diaspore + Fe–Ti-oxide matrix. Electron microprobe (EMP) studies (Feenstra, 1985, and in preparation) indicate that the compositions of minerals may differ significantly within samples or within thin sections. Millimetre- to centimetre-sized domains appear to have behaved as isolated chemical systems during metamorphism, and chemical equilibrium was approached on a local scale.

The absence of primary margarite in zone I and textural evidence indicate that margarite was unstable during the M_1 metamorphism. Margarite first appears in zone II at slightly higher grade than the corundum-in isograd and increases modally with grade. Margarite appears to have formed by complex continuous reactions, usually at the expense of chloritoid and calcite. As paragonite is the major Na-bearing mineral found in the diasporites, the Na content of margarite largely originated from incorporating paragonite in solid solution. In paragonite-free samples muscovite must have supplied the Na contained in margarite. EMP data (Feenstra, 1985, and in preparation) indicate that chloritoid which has partially reacted to margarite becomes enriched in Mg and associated Ti-haematite in ilmenite component. This and reaction textures indicate that the main margarite-producing reaction in zone II is of the form

Fe–Mg-chloritoid + calcite ± paragonite +
Ti-haematite + rutile = (Na)margarite + Mg-richer
chloritoid + Ti-richer haematite + CO_2.   (1a)

In zone III, replacement of chloritoid by margarite is more extensive and occasionally complete. Here margarite formation can be approximated by the reaction

chloritoid + calcite ± paragonite + Ti-haematite
= (Na)margarite + chlorite + corundum + magnetite
+ ilmeno-haematite + CO_2.   (1b)

Other local growth of margarite took place in zones II and III at the expense of M_1 kyanite and M_1 clinozoisite–epidote. In the $CaO–Al_2O_3–SiO_2–H_2O–CO_2$ (CASHC) system this margarite formation is described by the following two reactions:

kyanite + calcite + H_2O = margarite + CO_2 (2)

clinozoisite + kyanite + corundum + H_2O
= margarite.   (3)
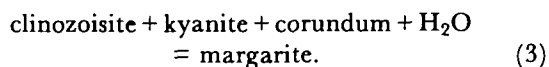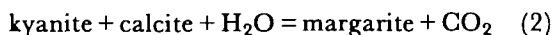
Feenstra & Maksimovic (1985) showed that the average CaO content of emeries is higher than that of diasporites (0·82 and 0·29 wt % CaO, respectively). This chemical difference, together with textural observations, provides evidence that part of the calcium contained in margarite was introduced from the surrounding marbles during metamorphism.

As all reactions described above are CO_2 producing or H_2O consuming, the appearance of margarite in zone II may have been triggered and catalysed by the transformation of diasporite into emery [according to the reaction $(2AlO(OH) = Al_2O_3 + H_2O]$, which generated large quantities of water-rich fluid in the metabauxite lenses.

Although prograde margarite is found up to the sillimanite-in isograd, its modal amount decreases with increasing grade from the middle of zone IV onwards (Figs 2 and 3). The margarite gradually breaks down according to the (CASH) reaction

margarite = anorthite + corundum + H_2O.   (4)
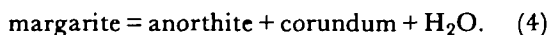
Many metabauxites in zone IV contain both margarite and plagioclase; the minerals are found in contact with one another or in separate parts of samples or deposits. Plagioclase grains are typically anhedral and poikiloblastic with ubiquitous corundum and Fe(–Ti)-oxide inclusions. Polysynthetic twinning of the plagioclase is common.

Texturally, three main types of margarite can be broadly distinguished. The first type is fine grained, occurring as a matrix mineral, particularly in the Si-rich metabauxite. It is most abundant in the metabauxites from zones II and III, but is also found in zone IV, particularly in the outer rims of the lenses. The matrix margarite, which grew in part syn-tectonically, is commonly intergrown with other white micas.

The second margarite type is medium grained, and forms post-tectonic sheaf-like aggregates. Some aggregates are monomineralic, but others contain interstratified muscovite, chlorite and/or biotite. This aggregate type is characteristic of the metabauxites in zone IV, but also occurs locally in deposits from zones II and III. Microstructural criteria indicate that aggregate margarite formed later during the M_2 event than did matrix margarite. The post-tectonic aggregate margarite may have developed partly through amphibolite-grade recrystallization of greenschist-grade matrix margarite. Another part may have grown with the aid of calcium introduced from the marbles during the M_2 event, as is suggested by geochemical studies (Feenstra & Maksimovic, 1985). Petrographic distinction between M_2 aggregate and retrograde margarite is not always easy. The most important criteria used for discrimination are that primary margarite is texturally related to peak M_2 minerals such as biotite and staurolite, whereas retrograde margarite is closely associated with secondary minerals or replaces primary minerals, particularly plagioclase. The EMP work indicates that most retrograde margarite is compositionally close to end-member margarite (see Mineral Chemistry section).

The third margarite type occurs as coarse-grained flakes in extensional veinlets, where it largely formed with the aid of introduced calcium and silica. The veinlet type was largely disregarded in this study; only some data for it from zone V have been included. The veinlet margarite is ubiquitous in the metabauxites of zone V but also occurs in the other zones. In zone V deposits, up to centimetre-size margarite flakes are commonly associated (partly intergrown) with coarse retrograde Fe-rich chlorite. As the upper thermal stability of margarite was clearly exceeded in zone V during M_2, all margarite must be of retrograde origin. Many margarite veinlets in deposits of the other zones are monomineralic but some veinlets contain retrograde minerals such as diaspore, chlorite, tourmaline, coarse rutile and magnetite. Although the time of margarite formation in monomineralic veinlets is difficult to constrain in zones I–IV, in analogy with zone V most veinlet margarite may be retrograde.

Muscovite is present in all metamorphic zones. On the basis of microstructural criteria and to a lesser extent by chemical data (see subsequent section), a distinction between M_1- and M_2-formed muscovite can be made. The M_1 type, which dominates in

zones I–III, occurs as coarse flat crystals that may display somewhat resorbed grain boundaries and in some cases are kinked and bent. In the lower and middle part of zone IV (zones IVl and IVm), relict M_1 muscovite has locally been preserved. No M_1 muscovite was found in the upper part of zone IV (zone IVu), indicating that M_1 muscovite did not survive a middle amphibolite-grade overprint.

M_2 muscovite occurs as medium-grained, commonly undeformed flakes. In zones IVl and IVm, M_2 muscovite is typically developed in the domains rich in other M_2 minerals such as margarite, plagioclase, biotite and staurolite, where muscovite became involved in reactions producing these minerals. Metabauxite with abundant M_2 minerals (e.g.

samples B492B, 113-3 and 24K4A; see Table 1 and Fig. 4) probably contains exclusively M_2 muscovite. On the other hand, in metabauxite showing only little development of typical M_2 minerals (apart from corundum, Fe–Ti oxides and some margarite), e.g. kyanitites and commercial emery, the M_1 muscovite still appears to dominate (e.g. samples 112A, 116E and 116F). Several samples of zones IVl and IVm show microstructural evidence for the presence of both M_1 and M_2 muscovite (e.g. 150B, 106-2 and 24L). In these samples, M_1 muscovite is marginally replaced by finer-grained M_2 muscovite, but more characteristically both muscovite generations occur in separate parts of the thin sections.

Paragonite, which is principally an M_1 mineral, is

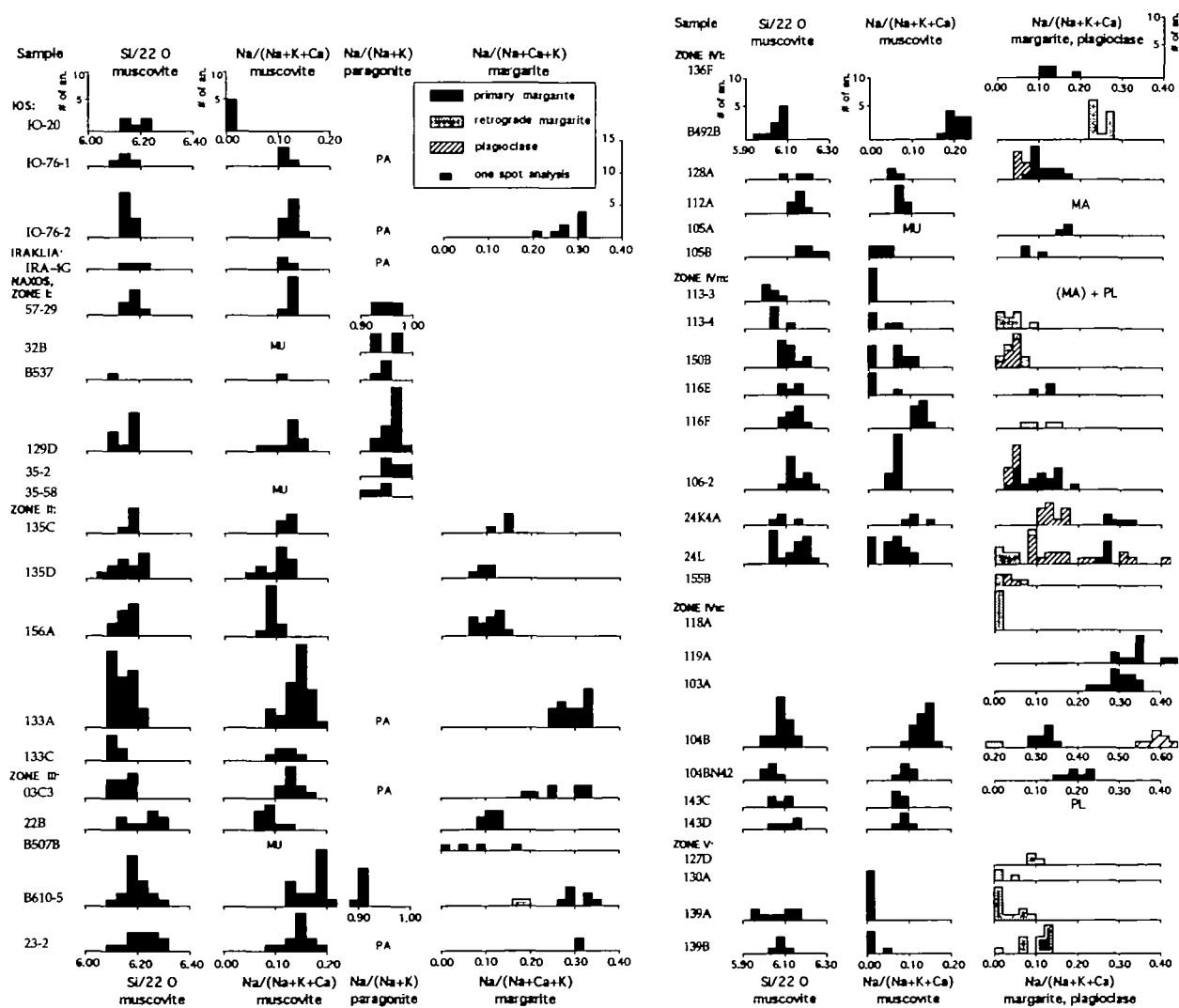Fig. 4. Si content of muscovite (atoms per 22 oxygens) and molar X_{Na} ratios of coexisting white micas and plagioclase in metabauxitic rocks studied from Naxos, Ios and Iraklia. Samples are approximately arranged in order of increasing metamorphic grade (refer to Figs 1 and 2 and Table 1). Zone IVl, lower part of metamorphic zone IV; zone IVm, middle part of zone IV; zone IVu, upper part of zone IV.

fairly common in the diasporites (Table 1). Paragonite and muscovite are commonly intergrown on a small scale in the diasporites. Especially in samples where one of the micas predominates modally over the other, it may be impossible to analyse the minor phase by microprobe (see Fig. 4). An additional problem in calcite-bearing diasporites is that white micas are locally intergrown with thin (<0.3 μm thick) calcite lamellae, which may contaminate EMP analyses of the micas. In zone II, the paragonite content of the metabauxites diminishes because the growth of margarite depletes the rocks in paragonite by including it in solid solution. Some paragonite persists up to zone III, but at higher grades all sodium in the emeries is contained in minerals such as margarite, muscovite, plagioclase and tourmaline.

ANALYTICAL METHODS

White micas and plagioclase were studied by routine electron microprobe methods in 42 metabauxite samples from Naxos, three diasporite samples from Ios and one from Iraklia (Table 1; Fig. 4). The rocks investigated from Naxos cover almost the complete metamorphic interval on the island. The metabauxites from Ios and Iraklia have experienced comparable P–T conditions to those in zone I of Naxos (Van der Maar & Jansen, 1983; Feenstra, 1985). Mineral assemblages in all samples studied are listed in Table 1. Naxos samples can be located in Fig. 2 with the aid of the coordinates given in Table 1. The localities of the samples from Ios and Iraklia are shown in Fig. 1.

Most of the EMP analyses were carried out on a Cameca Camebax electron microprobe, and the remainder with a Cambridge Geoscan or Cameca SX50 electron microprobe. The Cameca Camebax and Cambridge Geoscan microprobes are both equipped with a Link Systems energy-dispersive spectrometer and were commonly used at 15 kV in the EDS mode. A beam current of 2–4 nA and beam diameters between 1 and 8 μm were used for the analyses. Additional mica analyses were performed in several samples using wavelength-dispersive spectrometers on the Cameca electron microprobes, particularly to check for minor Ba, Rb, Sr, Cr and Ni contents. Structural formulae of white micas were calculated on the basis of 22 oxygens, with total iron expressed as ferric. Plagioclase formulae were calculated on an 8 oxygen basis. Because the compositional variation of the minerals exceeds the analytical accuracy of the microprobe in most samples (see Fig. 4), individual

spot analyses of the minerals instead of averaged values are shown in most diagrams. (Electron microprobe analyses of margarite, muscovite, paragonite and plagioclase are available from the author on request.)

Imaging techniques on the electron microprobe, particularly using back-scattered electrons (BSE), show that two or three different white micas are intergrown on a 0.1–1.0 μm scale in many greenschist-grade samples (zones I–III). In the samples of zone IV, interstratification of margarite and muscovite commonly is on a larger scale, allowing quantitative EMP analysis of the individual micas. Variable EMP analyses of apparently homogeneous micas in greenschist-grade rocks suggest that intergrowths of white micas could be present on a scale below the resolution of EMP imaging techniques ($< \sim 0.1$ μm). To investigate this possibility, several samples of zones II–III were selected for additional study by transmission electron microscopy (TEM) and analytical electron microscopy (AEM). The TEM–AEM studies (see following section) confirm that lamellar intergrowths of different white micas, particularly of margarite and paragonite, also occur on a 100–1000 Å scale in greenschist-grade rocks.

Electron microscopic investigations of white micas were conducted at the University of Manchester on a Philips EM400T operating at 120 kV. Regions containing micas suitable for TEM investigation were selected in thin sections, glued to 3 mm Cu grids and then prepared for TEM by Ar-beam thinning. Chemical compositions of coexisting micas were determined by analytical electron microscopy (EDAX spectroscopy) using the thin film approximation of Cliff & Lorimer (1975) and Lorimer (1987). The technique allows quantitative chemical microanalysis with a spatial resolution down to ~ 200 Å. In his review paper on use of thin film X-ray microanalysis, Lorimer (1987; figs 8 and 9) included an example of the method by A. Feenstra & P. E. Champness (unpublished) applied to finely intergrown lamellae of margarite, muscovite and paragonite in a chloritoid–staurolite-bearing calcic metapelite from the Dalradian in Scotland (sample DAL43 in Fig. 14, below; sample DAL43 was kindly provided by Dr G. T. R. Droop, Manchester University, UK). The results clearly show that three micas with fixed compositions occur in the sample, and indicate that quantitative AEM and EMP analytical methods are in good agreement. Such a comparison can, of course, only be made if single-phase mica flakes large enough for successful EMP analysis can be found in the sample. For many samples that are lower in metamorphic grade than the Dalradian, this may be difficult or impossible.

Table 1: Mineral assemblages in metabauxitic rocks studied from Naxos, Ios and Iraklia (see Figs 1 and 2 for locations of samples)

Sample no.	Latitude	Longitude	Crn	Dsp	Ky	Pg	Ms	Mrg	Pl	Czo/Ep	Cal	Cld	St	Chl	Bt	Hc*	Tur	Other	Haem	Ilm	Mag	Rt
IOS ISLAND																						
IO-20	36°45'11"	25°16'14"		O			X				X	X								O			A
IO-76-1	36°44'05"	25°15'39"		R	X	O	X					X						A		X			O
IO-76-2	36°44'05"	25°15'39"		X	X	O	X	X				X	O†					A		X			O
IRAKLIA ISLAND																						
IRA-4G	36°50'36"	25°26'17"		X		O	X												Prl	X			O
NAXOS ISLAND																						
Zone I																						
67-29	36°57'40"	25°33'05"		X		O	O				X								X			O
32B	36°57'25"	25°28'00"		X		X	O												O			O
B537‡	36°57'25"	25°28'00"		O		X	O				X	X							O			O
129D	36°57'50"	25°28'05"		X		X	X				O								X			O
35-2	37°01'45"	25°33'45"		O		X					X								O			O
35-58	37°01'45"	25°33'45"	O	X		O	O				X								O			O
Zone II																						
135C	37°00'40"	25°31'00"	O	R	X		O	X		O		X						A		X			O
135D	37°00'40"	25°31'00"	O	R			X	X			O	X		(A)					X			O
156A	37°00'50"	25°31'05"	X		O		O	X				X							O			O
133A	37°01'50"	25°31'25"	R	R	X	O	X	O		O		O	O†			R	A		X			O
133C	37°01'50"	25°31'25"	R	R	X		O			O		O					A		X			O
Zone III																						
03C3	37°02'40"	25°30'20"	X			A	X	X		R		X		O			A		O		X	A
22B	37°02'40"	25°30'20"	R		R		X	X		O		X		O			A	Qtz	O		X	
B507B	37°02'40"	25°30'20"	O				O	X				X		X					O		X	
B610-5	37°02'40"	25°30'20"	R		X	O	X	[X]		X				O			A	Qtz	X			A
23-2	37°02'35"	25°30'00"	R		X	O	O	X		X			O†	A			A	Qtz	X		O	O
Zone IV																						
136F	37°01'00"	25°27'20"	X					X							X	A	A			O	X	
B492B	37°01'00"	25°27'20"	O				O	(O)				R	X	X				Ap		X		A
128A	37°02'05"	25°25'25"	X				O	X	X					X						X	X	A

Sample no.	Latitude	Longitude	Crn	Dsp	Ky	Pg	Ms	Mrg	Pl	Czo/Ep	Cal	Cld	St	Chl	Bt	Hc*	Tur	Other	Haem	Ilm	Mag	Rt
112A	37°06'10"	25°33'30"	X		X		X	O					A		O		A		X			A
105A	37°06'10	25°33'15"	R		X		X	X		O						A		X		O	A
105B	37°06'10"	25°33'15"	X		O		O	X						(A)	X	A	A	Ap	X		X	
Zone IVm																						
113-3	37°06'15"	25°32'55"	X				O	(O)	X				O	(O)	X	A			O	O	X	
113-4	37°06'15	25°32'55"	X				O	(X)							O				O		X	
150B	37°06'15"	25°32'55"	X		O		X	(O)	X				X		X		A		O	O	X	
116E	37°07'20"	25°33'40"	O		X		X	X		X				O				Ap	X		O	A
116F	37°07'20"	25°33'40"	O		X		O	(X)		R					O				X			
106-2	37°07'45"	25°34'00"	X				X	O	O	O			A		O		A		X		X	
24K4A	37°07'10"	25°33'20"	X				O	O	X				X	O					O	O	X	
24L	37°07'10"	25°33'20"	O		X		O	[O]	X	O	O§		A		X	A	A	Ap	O		O	A
155B	37°06'20"	25°32'30"	X	(A)			O	(O)	X					(A)	X	A		(Hö)¶		O	X	
Zone IVu																						
118A	37°08'10"	25°33'00"	X	(O)				(X)								(A)	(X)				X	(O)
119A	37°08'05"	25°32'55"	X					X					O	O		A					X	
103A	37°09'40"	25°33'45"	X		O			O		(O)					X	A				O	X	
104B	37°11'40"	25°32'35"	X				X	[O]	X	A					O		A			O	X	
104BN42	37°11'40"	25°32'35"	X				X	X						O			A			O	X	
143C	37°11'40"	25°32'35"	X		X		X	O					O		O		A			O	X	
143D	37°11'40	25°32'35"	X				X			A			A		O		A			O	X	
Zone V																						
127D	37°06'25"	25°30'40"	X	(O)				(X)		(O)			R	(X)	O	(A)	(O)	Ap		O	X	
130A	37°07'25"	25°30'55"	X					(X)	X**	(O)				(X)	R	X				O	X	
139A	37°08'25"	25°31'05"	X				O	(X)				(O)		(X)				Grt		O	O	
139B	37°08'25"	25°31'05"	X				O	(X)				(O)		(X)				Grt		O	X	

Mineral abbrevations used are according to Kretz (1983); X, major mineral; O, minor mineral; A, accessory mineral; R, relict mineral, mostly occurring as inclusions; (....), retrograde occurrence; [....] , primary as well as retrograde occurrence.
*Solid solution of hercynite, gahnite and spinel.
†Zincian staurolite.
‡Samples beginning with B were collected by J. Ben H. Jansen.
§Calcite is only in contact with anorthite, biotite, muscovite, corundum and Fe–Ti-oxides
¶Hö, Högbomite.
** Plagioclase is strongly altered.

TEM–AEM STUDIES OF FINE-SCALE MICA INTERGROWTHS

Transmission electron micrographs and BSE pictures representative for samples of zone II (133A) and zone III (B610-5) are shown in Fig. 5. Corresponding AEM and EMP analyses are depicted for both samples in Fig. 6.

Sample 133A involves one of the lowest-grade margarite occurrences on Naxos. EMP work suggested that the paragonite content of its margarite is highly variable, ranging from 24 to 43 mol% (Fig. 6). TEM studies revealed, however, that semicoherent, 100–500 Å thick, paragonite interlayers are fairly common within the margarite grains (Fig. 5a and b). Muscovite grains, on the other hand, appear to be free of very thin (<500 Å thick) paragonite or margarite layers, but may be intergrown with margarite on a 0·1–1·0 mm scale (Fig. 5a and b). Single-phase margarite and muscovite regions large enough for AEM analysis could easily be found in sample 133A. Muscovite compositions determined with AEM are in accord with the EMP data. AEM analyses of margarite gave compositions with 22–31 mol% paragonite component, so that EMP analyses giving higher paragonite content are interpreted to result from incorporation of thin paragonite lamellae in the analysed spots (Fig. 6). Such paragonite lamellae are below the resolution of BSE imaging on the electron microprobe. Quantitative AEM analysis of the 100–500 Å thick paragonite lamellae in 133A was unsatisfactory. A rather intense electron beam is needed to generate sufficient X-ray intensity for the EDAX detector from such thin lamellae, resulting in considerable sodium loss. Nevertheless, the occurrence of paragonite interlayers can be inferred (a) from the fact that Na peaks characteristic for paragonite were present during the early stages of EDAX spectrum collection (counting times were 100–200 s) and (b) from the typical paragonitic Si/Al obtained. The latter suggests that although Na evaporates considerably during the analysis, the Si/Al ratio of the mica remains essentially unchanged. A further criterion to distinguish paragonite from margarite and muscovite by TEM is the observation that paragonite is more sensitive to radiation damage than are the Ca- and K-micas. Although HRTEM has proven to be a very useful technique to identify fine-scale interlayering of sheet silicates with markedly different basal spacings (e.g. 10 Å biotite alternating with 14 Å chlorite; Veblen & Ferry, 1983), high-resolution lattice imaging of the basal (001) mica planes is not diagnostic in the present

study as all three micas have the same $2M_1$ crystal structure with only slightly different basal spacings.

TEM and EMP investigation of sample B610-5 (zone III) reveals interstratification of all three micas on scales of 0·1 μm to several micrometres (Fig. 5c and d). Single-phase flakes of margarite, muscovite and paragonite that are coarse enough for EMP analysis were found in the sample. AEM data confirm that the EMP analyses closest to end-member Ca-, K- and Na-mica compositions correspond to one-phase compositions. Many other EMP analyses are from intergrowths of two or three micas. Sample B610-5 illustrates the problem that arises in EMP analysis of rocks containing submicron-scale intergrowths of various micas [see Ahn et al. (1985) and Shau et al. (1991)]. A major part of the mixed mica analyses shown in Fig. 6 could have been avoided by more careful selection of analysis spot using EMP imaging techniques. An additional complication of sample B610-5 is the presence of coarse retrograde margarite occurring in veinlets, where it is associated with retrograde chlorite and rutile. EMP analysis shows that this type of margarite is closest to end-member in composition (Fig. 6).

TEM studies of Na-rich margarites of zone IV (samples 24K4A and 119A) support the conclusion that these are single-phase, as thin paragonite or muscovite interlayers were not observed. AEM and EMP analyses are compatible for these margarites.

MINERAL CHEMISTRY

Margarite

In common with the findings of other workers on margarite, reviewed by Frey et al. (1982) and Guidotti (1984), the observed compositional variation for Naxos margarites can be explained to a considerable extent by solution towards paragonite (Figs 4 and 7). The metabauxitic margarite contains up to $\sim$44 mol% paragonite component; its muscovite component is <6 mol%. The analyses of prograde margarites show somewhat bimodal distributions for Ca and Na (Fig. 7); primary margarite having $\sim$20 mol% paragonite in solid solution is scarce in the rocks studied from zone II to zone IVm. Primary margarite from zone IVu is generally high in Na. This may reflect that increasing paragonite component in margarite stabilizes margarite to higher temperatures (Chatterjee, 1974; Bucher & Frey, 1994, pp. 233–250).

In the great majority of rocks studied, margarite coexists with muscovite, and in the rocks of zones IV and V frequently with biotite as well (see Table 1). The few rocks lacking a K-buffering phase contain margarite that is fairly low in K. The fact that mar-
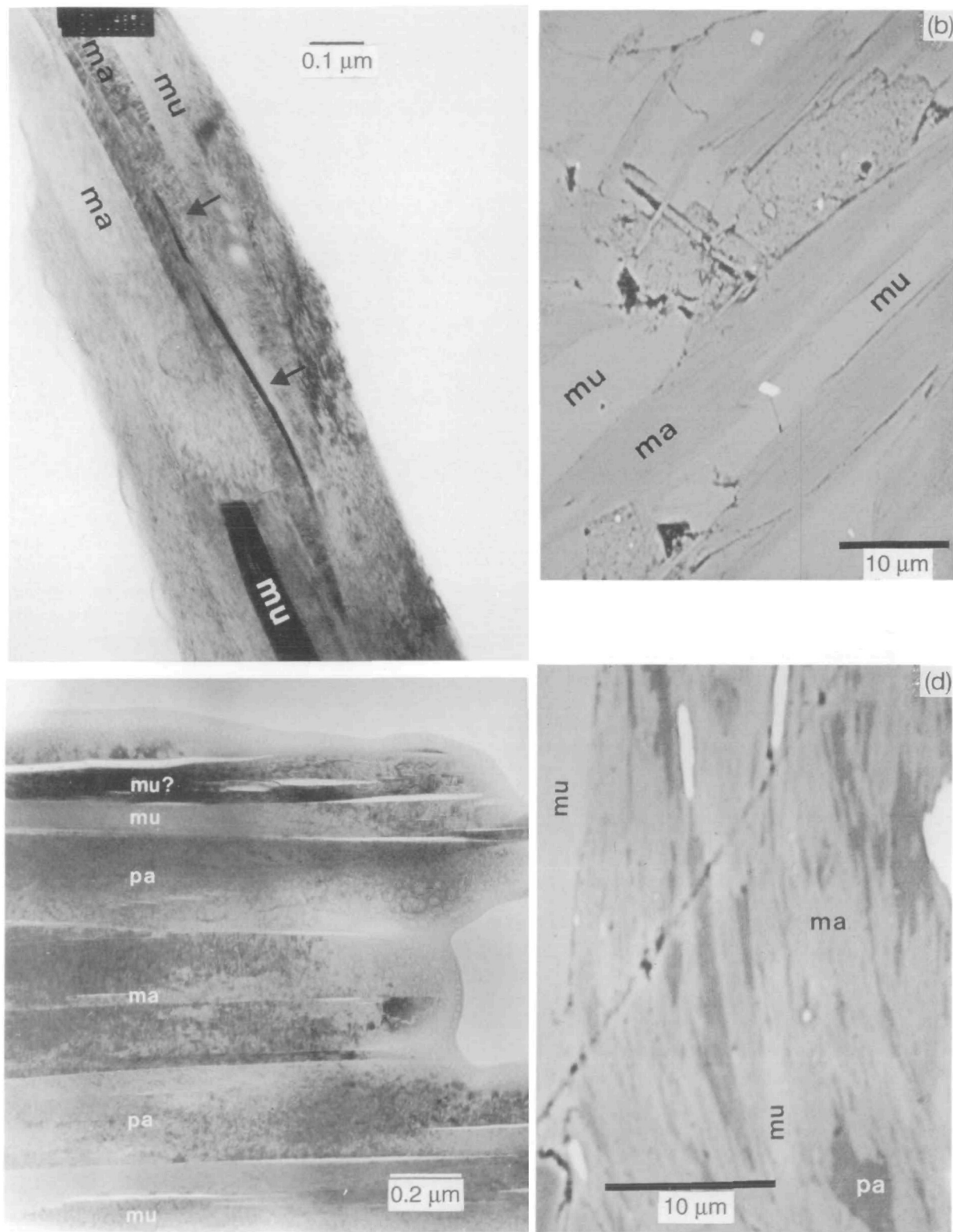
Fig. 5. Intergrowths of white micas in metabauxitic rocks of Naxos. (a) Transmission electron micrograph showing semi-coherent intergrowths of muscovite (mu) and margarite (ma) along their basal planes (sample 133A). The arrows indicate an ~100 Å thick paragonite (pa) lamella (black) within margarite (see text). The three small elliptical white spots in the muscovite flake on the right are beam-damaged regions owing to AEM analysis. (b) BSE picture of 133A showing aggregate of margarite and muscovite. Margarite contains vaguely visible semi-coherent lamellae of paragonite (dark grey), whereas muscovite grains appear to be homogeneous. (c) Transmission electron micrograph showing submicron-scale intergrowths of muscovite, paragonite and margarite in sample B610-5. The splitting of mica layers along (001) planes is probably the result of mechanical stress induced during specimen preparation. (d) BSE picture of B610-5 showing intergrown paragonite (dark grey), margarite (middle grey) and muscovite (light grey).
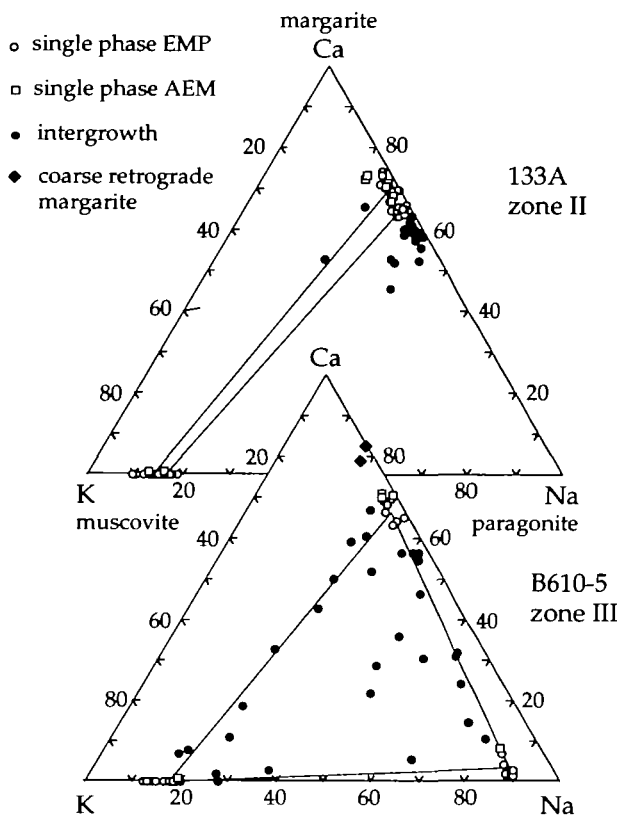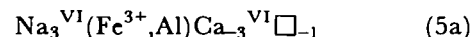
Fig. 6. Ca–Na–K diagram (atom %) depicting EMP and AEM analyses of white micas in samples 133A and B610-5. Tie-lines connect average compositions of micas in close contact. Margarite in sample 133A is locally interleaved with thin (<500 Å thick) paragonite lamellae which are too small for successful AEM analysis (see Fig. 5a and b).

garite of zones II and III tends to be somewhat higher in K than margarite of zones IV*l* and IV*m* (Fig. 7) appears to be surprising, because it would be expected that K solubility in margarite increases with metamorphic grade. The latter trend is shown by the zone IV*u* margarites that coexist with muscovite and contain 4–6 mol % muscovite component (note that several samples of zone IV*u* lack muscovite; Table 1). The comparatively high K content of margarite of zones II and III may partly result from a positive relationship between Na and K contents in margarite as indicated by Frey *et al.* (1982), as margarites analysed from zones II and III are on average richer in Na than those from zones IV*l* and IV*m*. In addition, it cannot totally be ruled out that contamination of margarite analyses with thin (<1000 Å thick) lamellae of muscovite causes the relatively high K content of the lower-grade margarite.
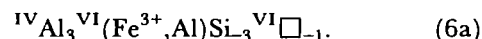
The (Ca + Na + K) histograms (Fig. 7) indicate that the interlayer is fully occupied in margarite, in contrast to muscovite and paragonite, which have in many cases (Ca + Na + K) <2·0 (see Figs 9 and 11, below). Octahedral Al in margarite shows a distribution centred on the ideal value of 4·0 for a di-octahedral mica. The (Fe + Mg) histograms essentially represent iron. Magnesium values were below the detection limit of the EDS analysis method [~0·03 atoms Mg per formula unit (p.f.u.)], except in three samples. The low Mg content of metabauxitic margarite, as compared with other margarites (Frey *et al.*, 1982), is a result of the high whole-rock Fe/Mg ratio of the bauxitic rock-type (Feenstra & Maksimovic, 1985). Whereas margarite in metamarls and calcic metapelites is commonly found in rather reduced (graphitic) assemblages, suggesting Fe to be predominantly ferrous (Frey *et al.*, 1982), metabauxitic margarite occurs in highly oxidized rocks. Up to the middle of zone III, margarite coexists with Ti-haematite, and at higher grades with magnetite + ilmeno-haematite/ferrian ilmenite (see Table 1). It is likely, therefore, that the margarite of the present study contains predominantly ferric iron. Hence margarite formulae were calculated with total iron expressed as ferric. This assumption is supported by recent Mössbauer spectroscopic investigations of metamorphic micas, showing that their $Fe^{3+}/\Sigma Fe_{tot}$ ratios, which are primarily a function of the oxygen fugacity prevailing at the time of crystallization, are high in oxidized rocks (e.g. Williams & Grambling, 1990; Guidotti & Dyar, 1991; Dyar *et al.*, 1993; Guidotti *et al.*, 1994*c*). For metapelitic muscovite, Guidotti *et al.* (1994*c*) obtained average $Fe^{3+}/\Sigma Fe_{tot}$ ratios of 0·45 in graphite-bearing and 0·67 in magnetite-bearing rocks.
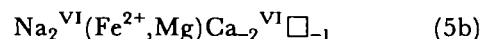
The precise substitutional mechanism for Fe in margarite is difficult to assess owing to its rather low Fe content. Figure 7 shows that the octahedral occupancy is higher than for an ideal di-octahedral mica, with up to 10% tri-octahedral component present. The primary margarites of zone IV*u* tend to be highest in tri-octahedral component, suggesting that this deviation from ideal margarite stoichiometry is promoted by increasing metamorphic grade. Possible substitutions counterbalancing the positive charge excess resulting from octahedral atoms (Fe, Mg, Al) in excess of 4·0 are

$$Na_3{}^{VI}(Fe^{3+},Al)Ca_{-3}{}^{VI}\square_{-1} \qquad (5a)$$

and

$$^{IV}Al_3{}^{VI}(Fe^{3+},Al)Si_{-3}{}^{VI}\square_{-1}. \qquad (6a)$$

In the case of ferrous Fe and Mg, the substitutions are

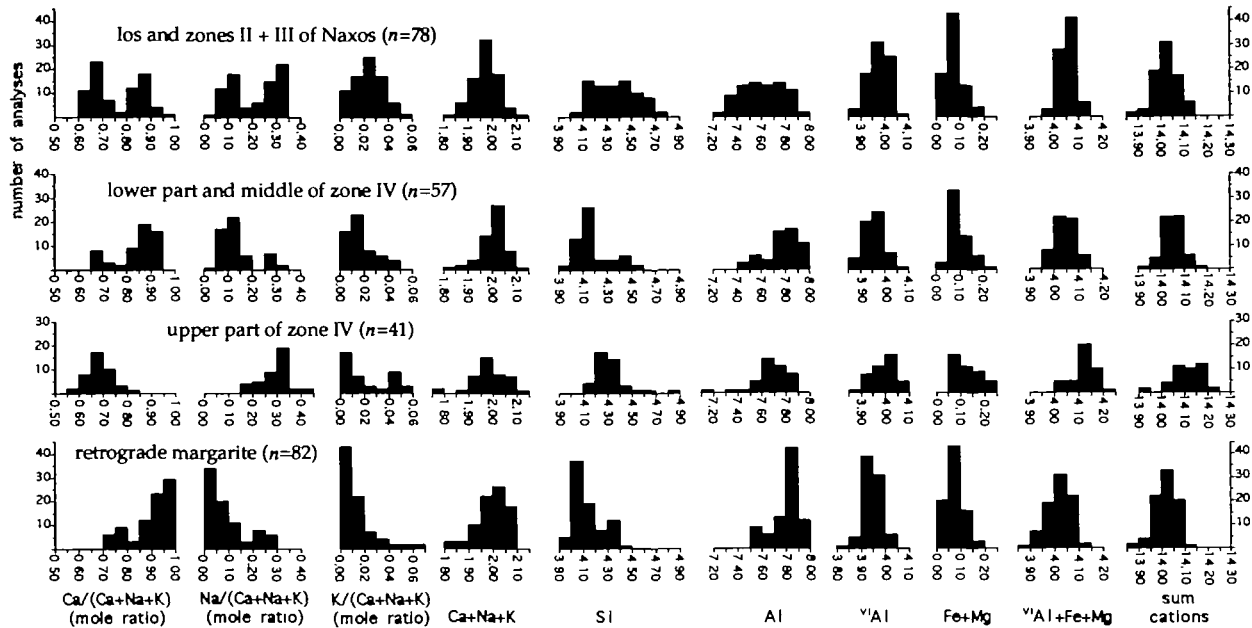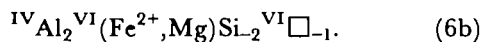$$Na_2{}^{VI}(Fe^{2+},Mg)Ca_{-2}{}^{VI}\square_{-1} \qquad (5b)$$

Fig. 7. Histograms showing the chemical variation of metabauxitic margarite (atoms per 22 oxygens). Total iron is expressed as ferric.

and

$$^{IV}Al_2{}^{VI}(Fe^{2+},Mg)Si_{-2}{}^{VI}\square_{-1}. \qquad (6b)$$

The above substitutions will lead to Na and ^{IV}Al excess (i.e. Ca and Si deficiency) in margarite relative to a stoichiometric mixture of end-members margarite, paragonite and muscovite, which follows the substitution

$$(Na,K)SiCa_{-1}Al_{-1}. \qquad (7)$$
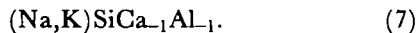
A plot of $(Na + K)$ vs Si (Fig. 8a) illustrates the Na excess and Si deficiency of the metabauxitic margarite relative to substitution (7); nearly all primary margarites plot above the substitutional line for (7). To test the applicability of substitutions (5a) and (5b), and (6a) and (6b), the octahedral cation sum was plotted vs $Na + K - Si + 4$, i.e. that part of $Na + K$ unbalanced by (7), in Fig. 8b and vs $^{IV}Al - Ca - 2$, i.e. that part of ^{IV}Al unbalanced by (7), in Fig. 8c. Comparison of the two plots shows that the octahedral cation sum is best correlated with $^{IV}Al - Ca - 2$ (Fig. 8c), suggesting that tri-octahedral Fe, Mg and Al may predominantly be balanced in the tetrahedral layer of the mica structure [substitution (6a)]. Excess ^{IV}Al and Na with respect to substitution (7), coupled with an octahedral occupancy higher than 4·0, appears to be a general feature for margarite chemistry (e.g. Frey *et al.*, 1982; Grew *et al.*, 1986). Substitution towards hypothetical end-members such as $Na_2(Al_4Fe_{0.67}^{3+}\square_{1.33})(Si_4Al_4)O_{20}(OH)_4$ and

$Na_2[Al_4(Fe^{2+},Mg)](Si_4Al_4)O_{20}(OH)_4$ therefore should be considered in understanding the mineral chemistry of natural margarite.

Incorporation in margarite of ephesite component, $Na_2(Li_2Al_4)(Si_4Al_4)O_{20}(OH)_4$, according to the substitution $Na^{VI}LiCa_{-1}{}^{VI}\square_{-1}$, will also lead to excess Na relative to substitution (7). Schaller *et al.* (1967) reported 0·19 wt % Li_2O (~ 5 mol % ephesite component) for a metabauxitic margarite from Naxos. The margarite is probably of retrograde origin. The microprobe data of this study do not suggest that retrograde margarite has a high Li content because it is fairly close to stoichiometric end-member composition (Figs 7 and 8). Although metabauxites are suitable host rocks for ephesite, because the mineral is only stable in silica-under-saturated compositions (Chatterjee & Warhus, 1984), the primary margarite probably does not have an important ephesite component for the following reason. Li is not an element typically enriched during bauxitization. As margarite is an important constituent of the Naxos emeries, high whole-rock Li concentrations would generally be required to reach a substantial Li content in margarite.

Muscovite

The chemistry of muscovite from the various metamorphic zones is summarized in histograms in Fig. 9. As for margarite, total Fe was expressed as ferric. In all metamorphic zones, muscovite coexists with Ti-
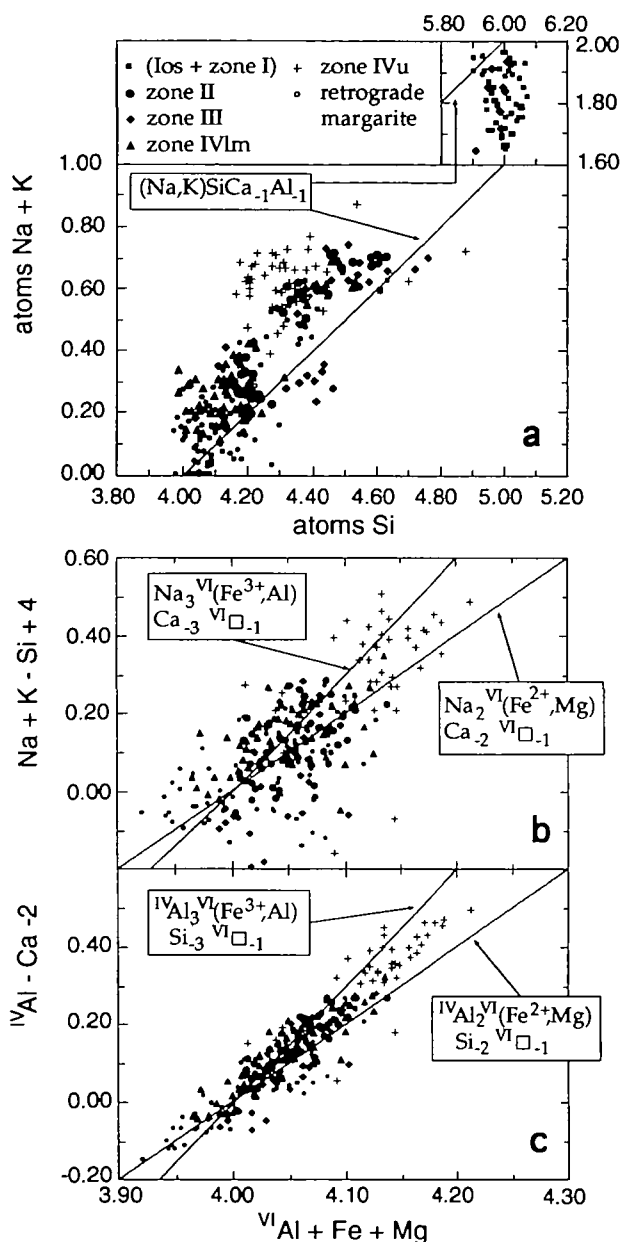
Fig. 8. Variation diagrams for metabauxitic margarite with labelled lines indicating suggested substitutions. Atoms are based on 22 oxygens. (a) (Na + K) vs Si. The right upper corner part of the diagram is for paragonite. (b) (Na +K – Si+4) vs (^{VI}Al + Fe+Mg). (c) (^{IV}Al – Ca – 2) vs (^{VI}Al + Fe + Mg).

and Fe^{3+}-saturating phases (rutile, haematite–ilmenite solid solution, magnetite) as well as an Al-saturating phase (diaspore, corundum). The Si-undersaturated bulk composition of the meta-bauxites is reflected in the comparatively low Si content of muscovite (5·95–6·32 atoms p.f.u.).

As in muscovite from metapelites (e.g. Guidotti, 1984), the (Na + K + Ca) sum in metabauxitic muscovite is typically <2·0 (Fig. 9) and the Ca content

is insignificant (<0·02 atoms p.f.u.). Low (Na + K + Ca) values could result from interlayer vacancies or unanalysed elements in the interlayer sites such as Ba, Rb, NH_4 and H_3O^+ (e.g. Voncken et al., 1987a,b; Loucks, 1991). Because EDS microprobe techniques have fairly high detection limits for Ba and Rb, the presence of these elements was checked with WDS techniques in some of the muscovites showing low interlayer totals. The WDS analyses gave negligible Ba and Rb for these muscovites, suggesting that both elements are unimportant in metabauxitic muscovite. As in margarite, Fe dominates over Mg in muscovite. The Mg/Fe of muscovite varies within the range 0–0·66, with most Mg/Fe values <0·4.

Examination of Figs 4, 9 and 10 shows that the diasporitic muscovites are compositionally similar to the muscovites in the emeries of zones II and III. A slight change in average chemical composition of muscovite is found in zones IVl and IVm: Si, Na and ^{VI}Al decrease, whereas K, Fe, Mg and Ti increase (Figs 4, 9 and 10). This overall compositional change is interpreted to result from pronounced growth of M_2 muscovite, largely by means of recrystallization of the predominantly M_1 muscovite at lower grades. Textures and chemical data indicate that M_1 muscovite is absent in zones IVu and V, implying that the M_1 type did not survive middle amphibolite-grade M_2 conditions.

Apart from interlayer NaK_{-1} exchange, the two most important substitutions in metapelitic muscovite causing deviations from ideal $K_2Al_4(Al_2Si_6)O_{20}(OH)_4$ composition are the Tschermak $^{VI}(Fe^{2+},Mg)Si^{VI}$-$Al_1^{IV}Al_{-1}$ and $^{VI}(Fe^{3+}AL_1)$ exchanges (Guidotti, 1984). The former leads to phengite $K_2[(Fe^{2+},Mg)Al_3](AlSi_7)O_{20}(OH)_4$, the latter to ferrimuscovite $K_2(Fe_2^{3+}Al_2)(Al_2Si_6)O_{20}(OH)_4$, and combination of both substitutions will give ferri-phengite $K_2[(Fe^{2+},Mg)Fe^{3+}Al_2](AlSi_7)O_{20}(OH)_4$ (see Fig. 10). A plot of (Fe + Mg) vs Si (not shown) indicates that nearly all metabauxitic muscovites contain much more (Fe + Mg) than required by the Tschermak exchange. This provides support for additional $^{VI}(Fe^{3+}AL_1)$ exchange, in accordance with the oxidized nature of the rocks. Di–tri-octahedral substitution, $^{VI}[(Fe^{2+},Mg)_3AL_2\square_{-1}]$, does not seem to be important, as octahedral occupancies cluster around 4·0 (Fig. 9). Some information on the relative importance of Tschermak vs $^{VI}(Fe^{3+}AL_1)$ substitution can be gained by means of graphical devices (Guidotti, 1984). Figure 10 shows that most muscovites from zones I–III plot between the muscovite–phengite and muscovite–ferriphengite joins or around the latter join, supporting combined Tschermak and $^{VI}(Fe^{3+}AL_1)$ exchanges. Muscovites
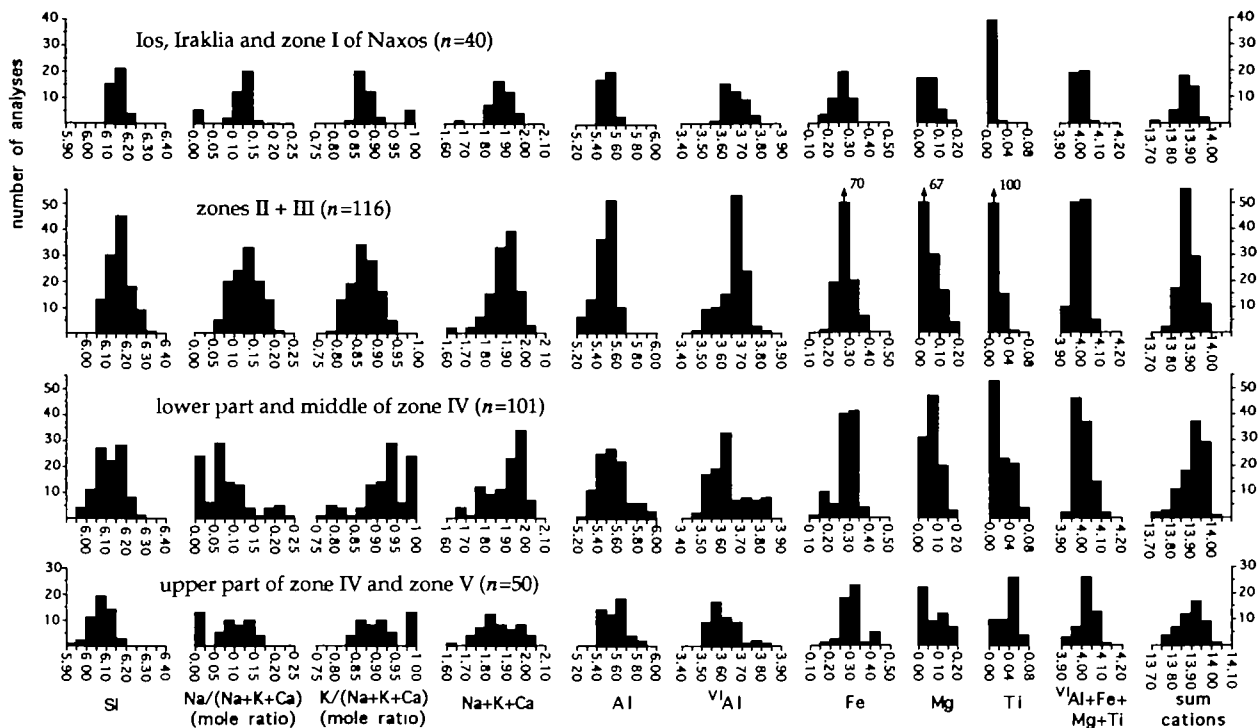
Fig. 9. Histograms showing the chemical variation of metabauxitic muscovite (atoms per 22 oxygens). Total iron is expressed as ferric.
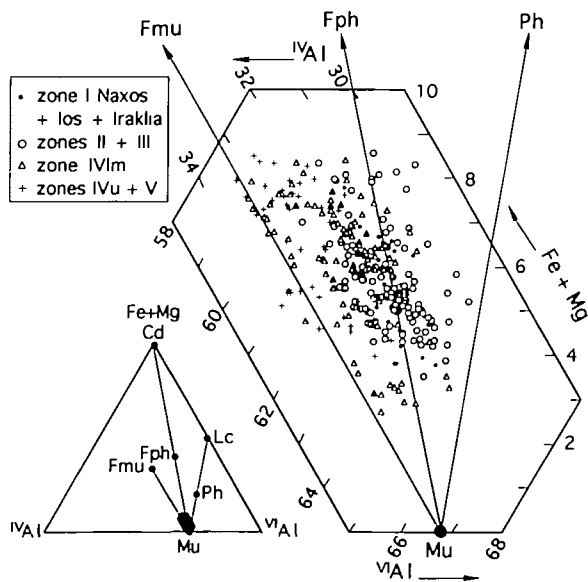

Fig. 10. $^{IV}Al-^{VI}Al-(Fe + Mg)$ diagram for metabauxitic muscovite (atomic proportions). Muscovite–phengite (Mu–Ph), muscovite–ferriphengite (Mu–Fph) and muscovite–ferrimuscovite (Mu–Fmu) exchange vectors are indicated in the diagram. Cd, celadonite, $K_2(Fe^{2+},Mg)_2Fe_2^{3+}(Si_8O_{20})(OH)_4$; Fmu, $K_2Fe_2^{3+}Al_2(Al_2-Si_6O_{20})(OH)_4$; Fph, $K_2(Fe^{2+},Mg)Fe^{3+}Al_2(AlSi_7O_{20})(OH)_4$; Lc, leucophyllite, $K_2(Fe^{2+},Mg)_2Al_2(Si_8O_{20})(OH)_4$; Mu, $K_2Al_4(Al_2-Si_6O_{20})(OH)_4$; Ph, $K_2(Fe^{2+},Mg)Al_3(AlSi_7O_{20})(OH)_4$.

from zones IVu and V plot between the muscovite–ferriphengite and muscovite–ferrimuscovite joins, indicating that $^{VI}(Fe^{3+}AL_{-1})$ exchange dominates over Tschermak exchange at higher amphibolite grade. The large compositional variation for zones IVl and IVm analyses indicates that this group includes both M_1- and M_2-formed muscovites, the former being approximately similar in composition to the muscovites from zones I–III and the latter to those from zones IVu and V. In summary, the vast majority of the metabauxitic muscovites deviate from ideal muscovite composition by both phengite and $^{VI}(Fe^{3+}AL_{-1})$ exchange. M_1 muscovites commonly have higher phengite and lower ferrimuscovite components than M_2 muscovites, which, particularly in the most silica-poor (commercial) metabauxite, have included Fe predominantly by means of $^{VI}(Fe^{3+}AL_{-1})$ exchange.

The chemical trends found for metabauxitic muscovite appear essentially $P–T$ controlled, although obscured by variation resulting from bulk-compositional effects. Given their small compositional differences, which are occasionally within the analytical accuracy of the electron microprobe, classification of muscovite in M_1 and M_2 type on chemical criteria only is difficult, for the following reasons. Muscovite

displays a rather continuous compositional spread in the samples (Fig. 4), which may relate to various degree of M_2 recrystallization. The chemical differences for muscovites in samples of comparable M_2 grade may not only result from a different origin (M_1, M_2) but could also arise from differences in the mineral assemblage with which muscovite has equilibrated. These cannot be very pronounced, however, as muscovite coexists with similar Al-, Fe^{3+}- and Ti-saturating phases in virtually all samples (see Table 1). As discussed above, the Naxos metabauxites are highly inhomogeneous with regard to bulk-chemistry and mineralogy. Uniform metamorphic equilibrium was commonly attained only at a millimetre to centimetre scale (Feenstra, 1985). These facts seriously hamper a quantitative evaluation of the variables controlling the composition of muscovite in the metabauxites.

Paragonite

Paragonite is a regular constituent of the diasporites but its small grain size and strong interlayering with muscovite did not allow its quantitative analysis by EMP in all samples (Fig. 4). In zones II and III paragonite could only be analysed in sample B610-5 (Figs 4 and 6); in other emery samples the paragonite flakes were too small to permit measurement. They range in thickness from 100 Å to a few micrometres and are particularly interstratified with margarite.

Paragonite from zone I contains up to ~8 mol % muscovite and ~4 mol % margarite in solid solution

(Figs 4 and 11). Paragonite from zone III is richer in muscovite component (8–10 mol %). Like other paragonites (e.g. Ackermand & Morteani, 1973; Höck, 1974; Guidotti, 1984), the metabauxitic ones are low in Fe (<0·13 atoms p.f.u.) and the Si content is centred on the ideal value of 6·00 (Fig. 11). The (Na + Ca + K) sum ranges from 1·69 to 1·98, suggesting that it contains variable amounts of interlayer vacancies and/or unanalysed interlayer elements. Grew et al. (1986) considered ^{IV}Al in excess of the $Ca^{IV}Al$ $(Na,K)_{-1}Si_{-1}$ exchange to be typical for paragonite in corundum-bearing rocks from Antarctica. Such ^{IV}Al excess (Si deficiency) is not characteristic, however, of Naxos paragonites (Figs 8 and 11).

Plagioclase

Plagioclase occurs in the emeries of zones IV and V but chemical data are presented only for zone IV (Figs 4 and 12). Microprobe analyses of retrogressed plagioclase grains from zone V gave low totals and non-stoichiometric formulae and are considered unreliable.

Metabauxitic plagioclase is rather pure in composition, containing only subordinate amounts of K and Fe (Fig. 12). With the exception of the plagioclase in rock 104B (An_{38-46}), plagioclase is calcium rich (Figs 4 and 12). Compositional data and petrographic observations suggest that plagioclase with an anorthite content higher than ~85% is a homogeneous phase. The wide range in anorthite content (An_{59-91}) found in the chemically inhomogeneous
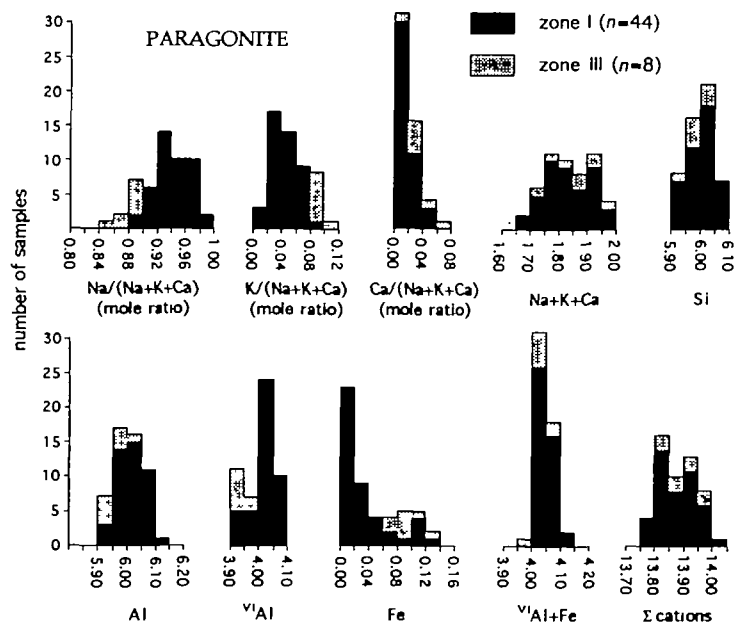

Fig. 11. Histograms showing the chemical variation of metabauxitic paragonite (atoms per 22 oxygens). Total iron is expressed as ferric.
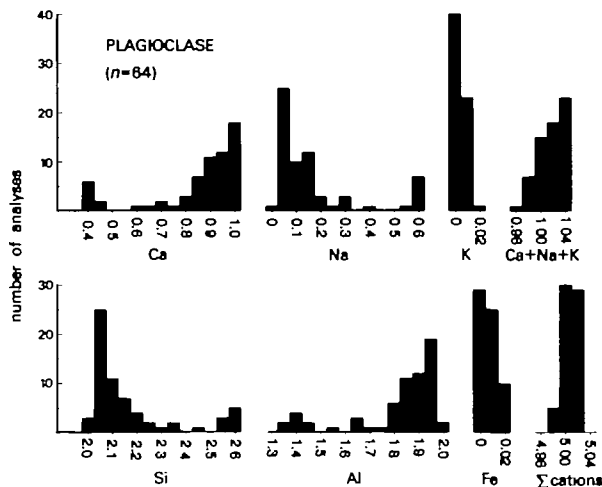
Fig. 12. Histograms showing the chemical variation of metabauxitic plagioclase (atoms per 8 oxygens).

sample 24L (Fig. 4) probably results from submicroscopic intergrowths of calcic plagioclase (An85–90) with intermediate plagioclase. The present results compare with those of other studies of plagioclase crystallized at amphibolite facies conditions, which suggest that plagioclase with An > ~85 is a single phase, whereas compositions measured between ~An40 and ~An85 may largely consist of small intergrowths of chemically and structurally different phases (e.g. Grove et al., 1983; Smith, 1983; Carpenter, 1988).

Ca–Na–K PARTITIONING

The Ca–Na–K partitioning between margarite, muscovite and plagioclase in the metabauxitic rocks is depicted in Fig. 13. The vast majority of tie-lines connect average compositions of minerals in contact, or averages for the sample when minerals were homogeneous on the scale of a thin section (compositions of micas and plagioclase plotted in Fig. 13 are listed in the Appendix). All samples from zone I are devoid of margarite and are not included in Fig. 13. Readers are referred to Fig. 4 and Table 2 for the Na–K distribution between muscovite and paragonite in the diasporitic rocks.

The phase relations among the white micas resemble those among the feldspars (Guidotti, 1984), with very little mutual solubility between the Ca and K end-members and restricted solubility of the Na phase towards both the Ca phase (Pg–Mrg solid solution) and K phase (Pg–Ms solid solution). In contrast to the feldspars, where complete solubility exists at high grades in the plagioclase (Na–Ca) and alkali-feldspar (Na–K) series, the white mica solvi do

not close in natural rocks because the micas break down at conditions below the critical temperatures for the solvi.

Muscovite–paragonite (Ms–Pg) solvus geothermometry

The phase relations between muscovite and paragonite have been investigated experimentally and theoretically by numerous workers [e.g. Eugster et al., 1972; Chatterjee & Froese, 1975; Chatterjee & Flux, 1986; for recent reviews see Guidotti et al. (1994a) and Blencoe et al. (1994)]. Although the experimental studies agree that the Ms–Pg system is characterized by a solvus with a critical temperature >800°C that is asymmetric towards paragonite, results on the location of the solvus in P–T–X space deviate significantly and appear to be inconsistent with data for naturally coexisting K–Na mica pairs (e.g. Essene, 1989; Blencoe et al., 1994). This disagreement has recently led Guidotti et al. (1994a) to develop an Ms–Pg solvus based on quasibinary Ms–Pg pairs from natural, medium-P metamorphic rocks. In a following paper, Blencoe et al. (1994) reformulated the solvus data as geothermometric expressions that allow quantitative temperature estimates from quasibinary K–Na micas for rocks equilibrated at pressures between 2 and 8 kbar.

Table 2 compares equilibration temperatures for metabauxitic K–Na micas from Ios, Iraklia and Naxos obtained with the geothermometric expressions of Blencoe et al. (1994) with independent temperature estimates based on reaction isograds and mineral assemblages. Although XRD studies and/or BSE imaging confirmed the presence of both muscovite and paragonite in the samples listed in Table 2, small grain sizes did not allow EMP analysis of both micas in all samples. In the latter cases, only one of the three thermometric expressions of Blencoe et al. (1994), either Pg- or Ms-based, can be applied. Compositionally (Table 2), the metabauxitic micas largely satisfy the quasibinary criteria [Ca/(Ca + Na + K) < 0·05 in Pg; Si ≤ 6·2 and (Mg + Fe_{tot}) ≤ 0·35 atoms p.f.u. in Ms] as set by Guidotti et al. (1994a) in developing their natural solvus.

The temperatures for the diasporites of Naxos derived from Ms–Pg thermometry are, within uncertainty limits, largely consistent with independent temperature estimates from assemblages such as pyrophyllite–kyanite and kyanite–diaspore (zone I) and diaspore–corundum (defining the beginning of zone II). The two samples from Ios (Table 2) give temperatures falling at the lower range of independent temperature estimates for the
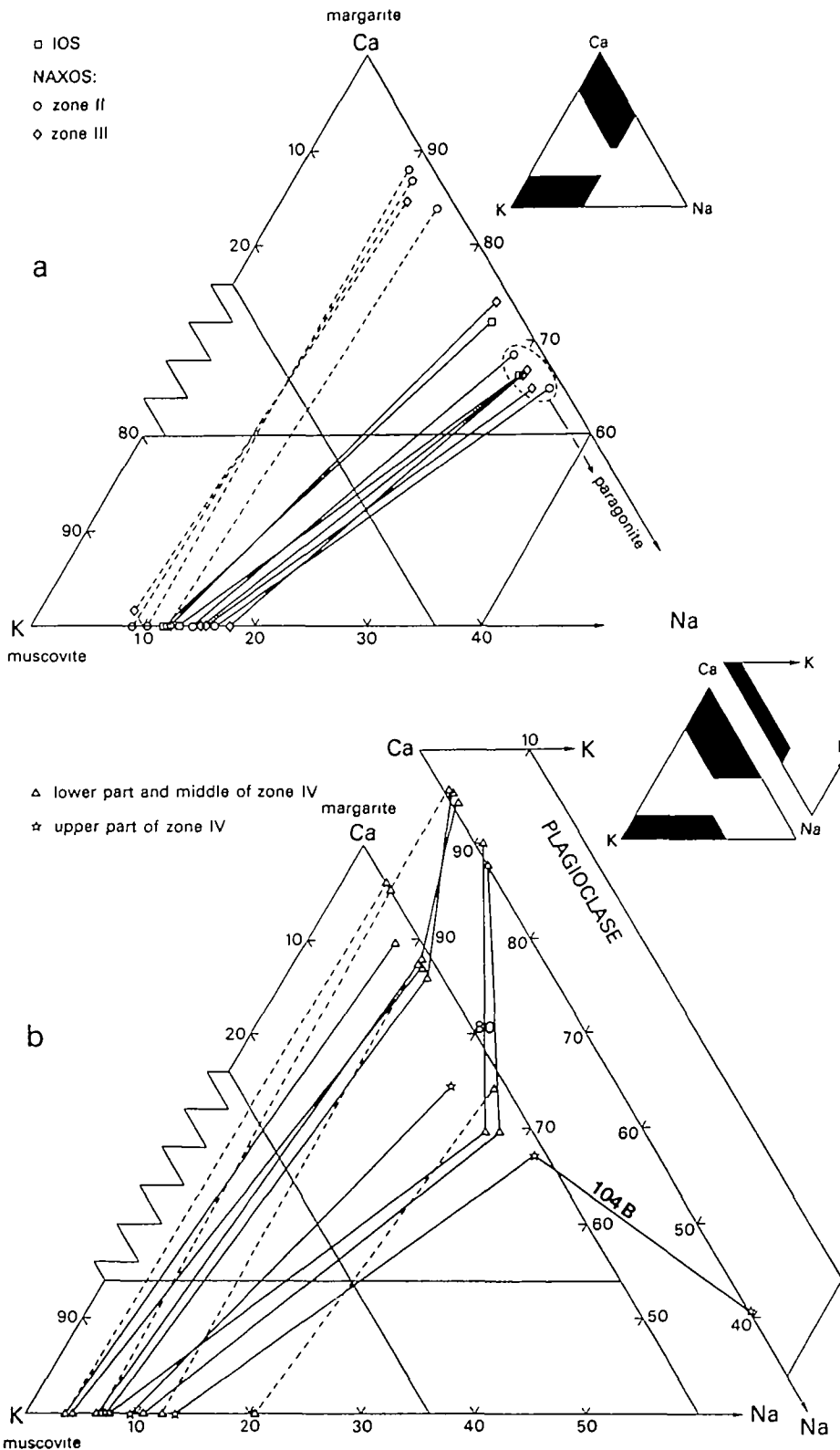
Fig. 13. Ca–Na–K partitioning between white micas and plagioclase in the studied metabauxites. Solid and dashed tie-lines indicate primary M_2 and non-equilibrium distribution, respectively (see text). Compositions of plotted micas and plagioclase are listed in the Appendix.

Table 2: Results of muscovite–paragonite thermometry

Sample	T-isog.*	Paragonite			Muscovite				T-Pgt	T-Mst	T-widtht
	(°C)	K/(K+Na)	X_{Ca}	No. an.	K/(K+Na)	Si	Fe+Mg	No. an.	(°C)	(°C)	(°C)
IOS											
IO-76-1	350–420‡	n.a.			0·885(12)	6·15(3)	0·29(3)	4		320(40)	
IO-76-2	350–420‡	n.a.			0·876(12)	6·15(2)	0·34(4)	10		350(40)	
IRAKLIA											
IRA-4G		n.a.			0·884(9)	6·17(5)	0·36(4)	3		330(30)	
NAXOS											
Zone I											
57-29	380	0·061(11)	0·028(16)	4	0·867(3)	6·17(2)	0·39(5)	6	330(80)	370(10)	350(30)
32B	400	0·070(6)	0·014(3)	3	n.a.				390(40)		
B537	400	0·058(6)	0·015(3)	3	0·886	6·12	0·34	1	310(40)	320	320
129D	410	0·053(14)	<0·01	8	0·861(6)	6·16(3)	0·27(5)	7	270(110)	390(20)	360(40)
35-58	420	0·065(19)	0·020(7)	4	n.a.				360(120)		
Zone II											
133A	460	n.a.			0·856(24)	6·15(4)	0·31(5)	32		400 (50)	
Zone III											
03C3	520	n.a.			0·862(16)	6·13(4)	0·33(5)	9		390(40)	
B610-5	520	0·095(6)	0·030(18)	8	0·823(21)	6·18(5)	0·40(7)	15	520(30)	470(40)	480(30)
23-2	530	n.a.			0·847(14)	6·22(4)	0·36(8)	11		420(30)	
Zone III/IV											
B492B	540				0·796(19)	6·05(4)	0·20(4)	11		510 (30)§	

X_{Ca}, mole fraction $Ca/(Ca+Na+K)$; no. an., number of EMP analyses on which averages are based; Si and (Fe+Mg) on the basis of 22 oxygens assuming total Fe to be ferric; values in parentheses for compositional parameters represent 1 SD in terms of the last digit(s) given; n.a., paragonite or muscovite present but not analysed.
*Estimated M_2 temperature on the basis of isograd pattern on Naxos (Jansen & Schuiling, 1976; Jansen, 1977; Feenstra, 1985).
†T-Pg, T-Ms and T-width are equilibration temperatures calculated with geothermometric equations (9), (10) and (11) of Blencoe et al. (1994), respectively based on K/(K+Na) of paragonite, muscovite, or both micas. Values in parentheses represent uncertainties in T based on SD in K/(K+Na).
‡M_1 conditions 9–11 kbar, 350–400°C; M_2 conditions 5–7 kbar, 380–420°C (Van der Maar, 1981; Van der Maar & Jansen, 1983).
§Minimum temperature, as muscovite does not coexist with paragonite.

island (Van der Maar, 1981; Van der Maar & Jansen, 1983).

For most Naxos samples of zones II and III, Ms–Pg solvus thermometry results in lower temperatures than inferred from biotite–chlorite–muscovite equilbria in metapelites (defining the beginning of zone III) and the first appearance of Fe-rich staurolite in metabauxites and metapelites (defining the beginning of zone IV). Exceptions are samples B610-5 and B492B, which give results consistent with the proposed M_2 metamorphic gradients for Naxos (see Table 2). The temperature obtained from the composition of muscovite in the latter sample, containing Fe-rich staurolite and chloritoid but lacking paragonite, should be considered as a minimum temperature.

The low Ms–Pg solvus temperatures suggest that the Na–K partitioning between the micas does not reflect peak M_2 conditions in several samples of zones II and III. As supported by microstructural observations and EMP data (muscovites in zones II and III have similar compositions to those in zone I), muscovite in particular may have retained its initial (high-P) M_1 composition. Close inspection of Table 2, excluding samples B610-5 and B492B, reveals that the results of Ms–Pg thermometry are

essentially uncorrelated with the M_2 isograd pattern on Naxos, providing additional support that chemical equilibrium between muscovite and paragonite has not been approached during M_2. Given that muscovite and paragonite in zones I–III may predominantly be of M_1 origin, the solvus thermometer of Blencoe et al. (1994) has been applied near the upper pressure limit calibrated for ($P \sim 9$ kbar during M_1). This could lead to underestimated temperatures, because the Ms–Pg solvus opens with increasing pressure. In particular, the muscovite limb shifts to more K-rich compositions because pressure-induced increase of octahedral Fe + Mg hinders incorporation of Na in muscovite for crystallochemical reasons (Guidotti et al., 1994b). The metabauxitic micas deviate, however, only slightly from the Ms–Pg binary, so that this effect can only be minor. Furthermore, the derived temperatures of 350–420°C are in reasonable agreement with independent, rather poorly constrained, M_1 temperature estimates (Feenstra, 1985, and in preparation).

Sample B610-5 from zone III yields a mica solvus temperature compatible with the proposed M_2 conditions. In the sample, which was also studied by TEM, all three white micas typically form subparallel intergrowths on a 0·1–10·0 μm scale (Fig. 5c and d), suggesting that they may be cogenetic. Unfortunately, owing to the general absence of paragonite in the samples of zones IV and V, it could not be tested whether Ms–Pg solvus thermometry yields M_2-consistent temperatures at amphibolite-grade conditions. Finally, it may be noted that the results obtained with the Blencoe et al. (1994) calibration are in much better agreement with the accepted metamorphic conditions for Naxos than those obtained with previous Ms–Pg solvus thermometers (e.g. Eugster et al., 1972; Chatterjee & Froese, 1975; Chatterjee & Flux, 1986). Of these, the Chatterjee & Flux (1986) calibration generally yields unrealistically low temperatures (at least 100°C too low), whereas the other experimental and theoretical calibrations commonly overestimate temperatures (see Blencoe et al., 1994).

Margarite–paragonite

The Mrg–Pg binary has received much less experimental attention than the Ms–Pg join and was studied only by Franz et al. (1977). Their synthesis experiments suggest the existence of an asymmetric miscibility gap (Na solubility in margarite is greater than Ca solubility in paragonite) along the join at temperatures below 600°C (see Fig. 14).

Coexisting margarite and paragonite could be analysed by EMP only in sample B610-5 (Figs 4 and 6). Several margarite-bearing samples of zones II and III contain additional paragonite grains that were too small for EMP analysis. In these rocks margarite should be Na saturated when both micas are in equilibrium. The mutual solubility between margarite and paragonite (Figs 4, 6, 13a and 14) is in all greenschist-grade samples considerably less than expected on the basis of the experimental work of Franz et al. (1977). The most Na-rich margarite at amphibolite-grade conditions contains up to 44 mol % paragonite in solution (sample 119A; see Fig. 14c). As this margarite does not coexist with paragonite, it must not necessarily show the maximum Na solubility at these conditions.

Margarite–muscovite

Margarite and muscovite show very little mutual solubility (Figs 7 and 13). Regarding the Na distribution between margarite and muscovite, the studied samples can be divided into two groups. In most samples (solid tie-lines in Fig. 13), margarite is about twice as rich in Na as the coexisting muscovite. In a smaller group of samples (dashed tie-lines) margarite and muscovite have a more or less similar Na content.

The margarite and muscovite that are connected with solid tie-lines in zone IV samples (Fig. 13b) display equilibrium textures with each other and with typical M_2 minerals such as anorthite, staurolite and biotite. Therefore the Ca–Na–K partitioning among them is believed to reflect peak M_2 equilibrium. Rocks of zone IV designated by dashed tie-lines show textural evidence that margarite is of retrograde origin. The roughly equal Na partitioning between margarite and muscovite in these rocks is therefore interpreted to represent non-equilibrium for peak M_2 conditions.

The interpretation of the Ca–Na–K partitioning among the white micas in the greenschist-grade samples is less straightforward (Fig. 13a). Here the rocks with dashed tie-lines ($X_{Na}^{Mrg}/X_{Na}^{Ms} \sim 1$) do not differ texturally from those with solid tie-lines ($X_{Na}^{Mrg}/X_{Na}^{Ms} \sim 2$), nor is there evidence that the samples of zones II and III have been severely affected by retrogression. The following causes for the dual Na distribution between margarite and muscovite at greenschist-grade conditions should therefore be considered:

(1) In the samples of zones II and III with dashed tie-lines, M_2 margarite and M_1-formed muscovite failed to equilibrate during the M_2 event, and muscovite largely preserved its original Na/(Na + K) ratio. This hypothesis is supported by Ms–Pg ther-

mometry, which for most samples of zones II and III yielded temperatures lower than inferred from other geothermometers for the M_2 event. Additional support is provided by the fact that three of the four samples showing equal Na distribution between margarite and muscovite are from zone II, where margarite first appears in the Naxos metabauxites. Here reaction rates may have been fairly low, the more so as geochronological studies suggest that the M_2 event may have been of fairly short duration (Wybrans & McDougall, 1986, 1988). By analogy with the primary tie-line configuration in zone IV samples (Fig. 13b), the Ca–Na–K partitioning in samples of zones II and III depicted with solid tie-lines (Fig. 13a) may indicate closer approach to M_2 equilibrium. However, it is important to note that for only one (B610-5) of the four studied Pg-bearing samples from zones II and III did Ms–Pg thermometry result in an M_2 temperature, whereas the other samples yielded temperatures too low for M_2. The moderately crosscutting solid tie-lines in the Pg-bearing samples (Fig. 13a) may reflect this lack of equilibrium between margarite and muscovite. On the other hand, it seems possible that the M_2 margarite could largely be saturated with paragonite component because texturally both micas are closely associated and their mutual solubility matches that of Ca–Na micas in rocks of comparable metamorphic grade as documented in other studies (Fig. 14; see discussion in following section). An apparently different reactivity in Pg-free and Pg-bearing samples during M_2 might be related to specific mica reaction mechanisms. In the former samples, the Na (and K) contained in margarite must essentially have been provided by muscovite, whereas in the latter paragonite may have played the dominant role as Na-supplying phase for the growing margarite, as is obvious from its disappearance in zone III. Also, preferential growth of margarite at the expense of paragonite is suggested by the thin (<500 Å thick) lamellae of paragonite in the lowest-grade margarite (Fig. 5a), which could be remnants of largely replaced M_1 paragonite grains.

(2) An alternative explanation for the observed Ca–Na–K partitioning in Fig. 13a is that besides a normal solvus relationship between margarite and paragonite (Franz et al., 1977), margarite shows a compositional gap around Ca/(Ca + Na) ~0.8 at greenschist-grade conditions. This extra gap in the Mrg–Pg series could be related to a discontinuity in crystal structure. Margarite has, at least up to a composition with 22 mol % paragonite in solution, nearly complete tetrahedral Si–Al ordering (Guggenheim & Bailey, 1978; Langer et al., 1981; Joswig et al., 1983), whereas the paragonite structure is tet-

rahedrally disordered (Lin & Bailey, 1984). Mixing of these structurally different members could possibly lead to an additional compositional gap at greenschist-grade conditions, as exists in the calcic portion of the plagioclase series.

Margarite–plagioclase–muscovite

Several samples of zone IV bear the assemblage Mrg + Pl + Ms (Fig. 13b). As in plagioclase-free rocks, primary margarite is higher in sodium than is muscovite. In most samples margarite is also clearly more sodic than the plagioclase. An exception is sample 104B, containing the most Na-rich margarite coexisting with plagioclase. In this rock, margarite is dinstinctly more calcic than plagioclase (see Fig. 13b). The divergent Ca–Na partitioning may relate to immiscibility at intermediate to calcic plagioclase compositions (Huttenlocher and Bøggild gaps; e.g. Smith, 1983; Grove et al., 1983; Wenk et al., 1991).

The first plagioclase occurring with margarite in the metabauxites is much more calcic and appears at higher metamorphic conditions than in quartz-bearing Mrg–Pl rocks from the Alps (Frey & Orville, 1974; Bucher et al., 1983; Bucher & Frey, 1994, pp. 233–250). In contrast to the observations made in quartz-bearing Al-rich marls, plagioclase commonly is more calcic than coexisting margarite in the corundum-bearing metabauxites. It is interesting that in the few Mrg–Pl–corundum rocks known from the Alps the plagioclase is also the more calcic phase (Frank, 1983; Bucher et al., 1983). The reversal in Ca–Na distribution between plagioclase and margarite in corundum-bearing rocks as compared with quartz-bearing ones might be a consequence of their Al-excess bulk composition and the comparatively high metamorphic grade of such rocks (A. Feenstra, in preparation).

Comparison with other studies

Rocks containing only margarite and paragonite as white micas seem to be rare, which may reflect the scarcity of the appropriate (K-poor) bulk compositions. Examples of coexisting margarite and paragonite in Ms-free rocks were reported by Ackermand & Morteani (1973) from Tyrol, Grew et al. (1986) from Antarctica and Enami (1980) from Japan (see Fig. 14). Metamorphic rocks containing Mrg + Pg + Ms appear to be much more common (e.g. Höck, 1974; Frey & Orville, 1974; Frey, 1978; Hoinkes, 1978; Guidotti et al., 1979; Frey et al., 1982; Okuyama-Kusunose, 1985; Lorimer, 1987; Yalçin et al., 1993). In many cases, reliable chemical data for
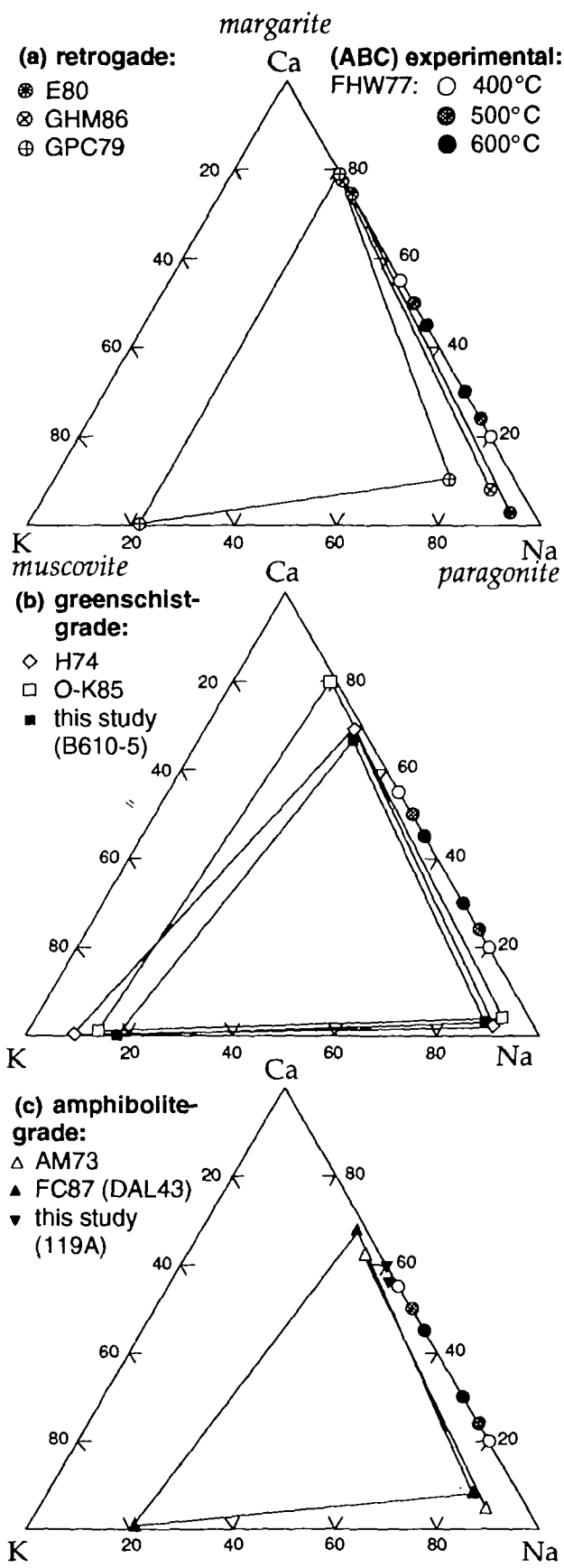
all three micas are, however, difficult to obtain because the micas are intimately intergrown on a scale beyond or near the resolution of the electron microprobe.

Figure 14 compares the Ca–Na–K partitioning among the white micas in Naxos sample B610-5 with a selection of literature data. Plotted samples contain either Pg + Mrg or all three white micas. Also shown (Fig. 14c) are the most sodian margarites found on Naxos at amphibolite-grade conditions. These margarites from sample 119A, which TEM investigations confirmed as single phase, do not coexist with paragonite and muscovite. It can be seen from Fig. 14 that paragonite coexisting with margarite contains $< \sim 10$ mol % margarite in solution. A similar restricted Ca solubility in paragonite is also evident from the compositional data for paragonite compiled by Frey et al. (1982) and Guidotti (1984). For the compiled data, the maximum solubility of paragonite in margarite amounts to ~ 34 mol % at greenschist-grade (Fig. 14b) and ~ 44 mol % at amphibolite-grade (Fig. 14c) conditions. The plotted data only suggest a slight increase in Na solubility in margarite with increasing metamorphic grade, implying that the margarite limb of the solvus may be rather steep. A similar increase of Ca solubility in paragonite at the other side of the solvus is not obvious from the data in Fig. 14. Like the Ms–Pg solvus, the Mrg–Pg solvus is asymmetric towards the side with the smallest volume (greater solid solution of Na in margarite than of Ca in paragonite) and is truncated at higher temperatures owing to formation of plagioclase. The breakdown of Ca–Na micas occurs, however, at significantly lower temperatures than that of K–Na micas (e.g. Bucher et al., 1983; Chatterjee & Flux, 1986; Bucher & Frey, 1994, pp. 233–250; A Feenstra, in preparation).

For both greenschist- and amphibolite-grade rocks the mutual solubility displayed by natural paragonite and margarite (Fig. 14b and c) is clearly less than that indicated by the experimental study of Franz et al. (1977) at 1–6 kbar. The retrograde margarite and paragonite from Antarctica (Fig. 14a), which formed by breakdown of staurolite at 300–370°C and 3–5 kbar (Grew et al., 1986), also show less miscibility than suggested by the experimental work. The difference between experiment and nature may relate to difficulties in establishing the precise size of the two-phase region in the synthesis experiments. Metastable phases and small, poorly crystallized, Mrg–Pg mixed layers may have formed in the experiments, which led Franz et al. (1977) to state that their results should be considered as a first approximation.

The Na distribution between margarite and muscovite depicted in Fig. 14 appears irregular. The lowest X_{Na}^{Mrg}/X_{Na}^{Ms} (~ 1) is found in the white mica pseudomorphs after andalusite studied by Guidotti et al. (1979), and the highest ratio (~ 3) in the greenschist-grade rock studied by Höck (1974). The other samples show X_{Na}^{Mrg}/X_{Na}^{Ms} between 1·4 and 1·7. The irregular tie-line pattern between margarite and muscovite may largely be related to the fact that for a given temperature the K–Na and Ca–Na mica solutions respond to pressure in different ways. Whereas it is clearly established for the Ms–Pg system that, owing to crystallochemical controls, increasing pressure decreases the solubility of Na in muscovite (Guidotti et al., 1994b), pressure may have little or even an opposite effect on the solubility of Na in margarite. Volume–composition data of natural sodic margarites compiled by Okuyama-Kusunose (1985) strongly scatter around the ideal mixing line between synthetic margarite and paragonite and do not allow conclusions on the size (and sign) of an excess volume at the margarite side of the solvus. The formation of highly sodic margarites at relatively high pressures during decompression of eclogite-facies rocks (e.g. Meyer, 1983; Smith & Kechid, 1983) supports, however, increasing Na solubility in margarite with rising pressure. If the Ca–Na–K partioning between the micas in Fig. 14 represents equilibrium, re-orientation of the Ms–Mrg tie-lines towards more sodic margarite and less sodic muscovite with increasing pressure finds support in the plotted data. The pseudomorphic micas (Guidotti et al., 1979), the greenschist-grade ones of Okuyama-Kusunose (1985), and probably also the retrograde Naxos margarite (dashed tie-lines in Fig. 13b), formed at low pressures. The micas

Fig. 14. Ternary molar diagrams comparing Ca–Na–K partitioning amongst white micas in (a) retrograde pseudomorphic occurrences, (b) greenschist-grade rocks and (c) lower amphibolite-grade rocks. Sources of plotted data: AM73, Ackermand & Morteani (1973); E80, Enami (1980); FC87 [sample DAL43; see fig. 9 of Lorimer (1987)], A. Feenstra & P. E. Champness (unpublished data); FHW77, Franz et al. (1977); GHM86, Grew et al. (1986); GPC79, Guidotti et al. (1979); H74, Höck (1974); O-K85, Okuyama-Kusunose (1985); B610-5, this study. Most data points are averages of microprobe analyses within a single sample; in some cases, comparable results for several samples have been replaced by an average for clarity (see the Appendix for more information). The amphibolite-grade rocks studied by Ackermand & Morteani (1973) and the pseudomorphic occurrences studied by Enami (1980) and Grew et al. (1986) are free of muscovite. Also shown are the most sodian margarites of this study (sample 119A, zone IVu) which do not coexist with paragonite or muscovite. The experimentally determined width of the miscibility gap in the margarite–paragonite series at 400, 500 and 600°C and 1–6 kbar (Franz et al., 1977) is shown for comparison on the Ca–Na baseline in all three diagrams.

described by Lorimer (1987) and in this study (sample B610-5) equilibrated at intermediate pressures ($P \sim 6$ kbar), and the greenschist-grade ones studied by Höck (1974) probably at the highest pressures, as reflected in the comparatively high Si content of the muscovite (Si = 6·37 atoms p.f.u.; see the Appendix).

The above conclusions should be considered as preliminary because the Ca–Na–K partitioning in the white mica plane is controlled by a complex interplay of P, T, rock composition and the opening and closing of three solvi. Additional detailed EMP, HRTEM–AEM and crystal-structural studies of Ca–Na–K micas from petrologically well-known rocks are needed to improve our understanding of their phase relations, volume–composition relationships, and solution properties. In new experimental work, careful characterization of run products by XRD, HRTEM–AEM and various spectroscopic methods may help solve existing inconsistencies with natural observations regarding the mutual solubility of Ca–Na–K micas.

IMPLICATIONS OF SMALL-SCALE MICA INTERLAYERING AND DIFFERENT WHITE MICA GENERATIONS IN POLYMETAMORPHIC ROCKS

Several results of this study are important for the petrogenetic interpretation of white micas in lower-grade metamorphic rocks. The first involves the common occurrence of submicroscopic intergrowths of Ca–Na–K micas in the greenschist-grade Naxos samples. Compositional data for metamorphic white micas that clearly fall within the miscibility gap depicted in Fig. 14 have regularly been reported in the literature. For example, Thompson et al. (1977) studied inclusions in a large garnet from the Gassetts schist (Vermont, USA) and measured margarite and paragonite with compositions $Mrg_{47}Pg_{52}Ms_1$ and $Mrg_{25}Pg_{73}Ms_2$ in adjacent inclusions. Recently, Vance & Holland (1993) made a detailed study of inclusions in a comparable garnet from the Gassetts schist, inferred to have grown during heating from 540 to 635°C and decompression from 9·7 to 7·2 kbar. The compositions of the mica inclusions, which are absent only in the extreme rim of the garnet, cover the complete Mrg–Pg join; however, a systematic compositional change with position in the garnet was not observed for the micas. As such mica inclusions may have been shielded from further reaction by the enclosing garnet, they may provide important information on miscibility relations among white micas near their upper stabilities. Unfortunately, the compositional mica data presented by Vance & Holland (1993), especially from the core of the garnet, cannot be consistent with the Ca–Na partitioning between margarite and paragonite displayed in Fig. 14. Sample B610-5 (from Naxos) and DAL43 (from Scotland) both equilibrated at metamorphic conditions (slightly down- and up-grade of the staurolite-in isograd) comparable with the core of the garnet studied by Vance & Holland (1993). In contrast to the Gassetts rock, in which complete solid solution between margarite and paragonite was assumed by the researchers, Ca- and Na-micas in samples B610-5 and DAL43 display only a restricted mutual miscibility. Both the Naxos and Scottish sample (Lorimer, 1987) were subjected to additional HRTEM–AEM investigations and used to demonstrate the problems involved in EMP analysis of micas intergrown on a (unnoticed) small scale. Like other unrealistic Ca–Na–K mica compositions (e.g. Yardley & Baltatzis, 1985; Stähle et al., 1986), the divergent Ca–Na mica compositions measured by Vance & Holland (1993) can probably best be explained by two-phase or three-phase intergrowths, which could be tested by additional HRTEM–AEM studies.

In low- to medium-grade metamorphic rocks (sub)coherent interlayering of Na- and K-micas on a submicron scale appears to be common, as documented in several TEM–AEM studies (e.g. Ahn et al., 1985; Lorimer, 1987; Shau et al., 1991). The fine-scale lamellar intergrowths are probably inherited from anchimetamorphic mixed-layer Ms–Pg (e.g. Frey, 1987) or early metastable Na–K mica having intermediate compositions (Jiang & Peacor, 1993). An alternative interpretation that the intergrowths could result from retrograde unmixing of metamorphic micas initially showing larger mutual solubility, as has been observed in the structurally related amphiboles, seems unlikely. Textural and petrological evidence such as the absence of small-scale white mica interlayering in amphibolite-grade Naxos samples does not lend support to this hypothesis.

The problem that the EMP beam is too wide to obtain single-phase compositions of white micas (or other phyllosilicates) seriously hampers the study of their phase relations in the lower ranges of metamorphism. If the problem is unrecognized, mixed analyses can easily lead to incorrect interpretations of phase relations and erroneous results for muscovite–paragonite and phengite geothermobarometry. As TEM–AEM studies are more complicated and time-consuming than routine EMP studies, the former cannot be performed on all rocks with suspected small-scale mica interlayering. Fortunately,

the sophisticated electron imaging techniques of modern electron microprobes allow the EMP analyst to obtain at least some information on (possible) mica interlayering. When coarser single-phase mica flakes are locally present in the sample, careful selection of analysis spot (e.g. by using BSE imaging) may result in the correct (single-phase) mica compositions, as was demonstrated in the present study (sample B610-5; see Fig. 6). If the mica interlayering is entirely beyond the resolution of the EMP or even occurs on a scale ($< \sim 0.1$ μm) invisible with common imaging techniques, then EMP analysis will inevitably integrate the various mica compositions, resulting in 'mixed' analyses (e.g. sample AF133A, Fig. 6). By measuring a large number of spots and plotting the analyses in compositional diagrams (e.g. Fig. 6 of this study; Petrakakis & Jawecki, 1995), the scatter of the data can be judged. When the measured micas display a large compositional variation and/or analyses have resulted in unrealistic compositions (e.g. Ca-rich muscovite, K-rich margarite, very Na-rich muscovite in high-P rocks) the data should particularly be interpreted with caution.

Another aspect of the present study is the occurrence of different white mica generations formed during polymetamorphism. On Naxos, early high-P, M_1 muscovite largely survived the greenschist-grade overprint of the medium-P, M_2 event. Owing to the Si-undersaturated bulk composition, which does not allow extensive Tschermak substitution, the metabauxitic M_1 and M_2 muscovite differ only slightly in composition and both types are best distinguished from a microstructural point of view. In the metapelitic rocks of Naxos, relict M_1 muscovite occurs up to the middle of staurolite zone IV and is distinctly more phengitic than M_2 muscovite (Andriessen, 1978; Wybrans & McDougall, 1986, 1988; A. Feenstra, unpublished data). Conventional K–Ar dating of metapelitic white micas from zones I–III (Andriessen et al., 1979) resulted in mixed M_1 and M_2 ages (48–20 Ma) with the ages decreasing with M_2 grade. Subsequent ^{40}Ar/^{39}Ar dating by Wybrans & McDougall (1986, 1988) generally confirmed up to zone IV the combined effect of the M_1 and M_2 events on the age patterns displayed by white mica.

Multiple populations of compositionally different K-micas formed at distinct P–T conditions are not only common in the rocks of the Cycladic realm (e.g. Schliestedt, 1986; Bröcker et al., 1993) but have also been documented in many other polymetamorphic terranes (e.g. Chopin & Maluski, 1980; Frey et al., 1983; Stöckert, 1985; Massone & Schreyer, 1987; Dempster, 1992; Scaillet et al., 1992; and references therein). As in the Cyclades, many examples are from rocks that have experienced an early high-P

event followed by a medium-P overprint at greenschist- to lower amphibolite-grade conditions. Such a P–T–t evolution may be reflected in zoned K-micas with phengite-rich cores and less phengitic rims (e.g. Stöckert, 1985; Schliestedt, 1986). Such chemical zoning and the preservation of distinct white K-mica generations, despite the fact that, as on Naxos, many of these rocks have experienced temperatures in excess of 500°C during the second event, document their sluggishness to homogenize and re-equilibrate in geological times (Chopin & Maluski, 1980; Massone & Schreyer, 1987; Dempster, 1992; Scaillet et al., 1992).

In natural rocks, the recrystallization of a particular mineral is controlled not only by its solid-state diffusion characteristics (mainly a function of T) but also by many other factors such as the presence or absence of grain boundary fluid and deformation. At the lower grades of Naxos, it was observed that M_2 muscovite formed preferentially in samples with ample development of other M_2 minerals (muscovite was involved in discontinuous M_2 reactions), whereas in samples of comparable grade having bulk compositions that were chemically less reactive during M_2 (kyanitites, commercial emery) M_1 muscovite largely persisted metastably. These observations imply that recrystallization and nucleation of muscovite is not primarily dictated by temperature but is driven by chemical reactivity and the presence of metamorphic fluid (virtually all prograde reactions in the metabauxites produce H_2O and/or CO_2). As the main mass of the metabauxite lenses is undeformed, and high-T, M_2-related deformation is largely confined to the outer rims of the lenses and thin (< 1 m thick) layers, deformation was probably not essential in controlling mica reactivity. A positive relationship between degree of deformation and mica reactivity (Chopin & Maluski, 1980) is lacking for the studied samples. In conclusion, the sluggishness of K-micas to homogenize and re-equilibrate during polymetamorphic events as documented in this and many other studies has important implications for using them for geothermobarometric and geochronological purposes (e.g. Chopin & Maluski, 1980; Massone & Schreyer, 1987). The present study generally emphasizes the need for careful petrographic, microstructural and microanalytical investigations of white micas to assess their equilibrium state in polymetamorphic rocks.

SUMMARY AND CONCLUSIONS

(1) Electron microprobe analysis of coexisting white micas in greenschist-grade rocks can be com-

plicated by the presence of mica interlayering on a scale below the resolution of the electron microprobe. Failure to recognize such small-scale interlayering may lead to wrong interpretations of mica phase relations as demonstrated by combined EMP and TEM–AEM investigations in this study.

(2) In contrast to muscovite and paragonite, which already existed during a first Alpine, high-P event affecting Naxos, margarite formed at the greenschist grade of the second, medium-P event. The metabauxitic margarite mainly deviates from end-member composition by including paragonite in solid solution (up to 34 mol % at greenschist- and 44 mol % at amphibolite-grade conditions). The muscovite content of the margarite is <6 mol %. Virtually all primary margarite contains more $(Na + K)$ than balanced by $(Na,K)SiCa_{-1}Al_{-1}$ exchange. This feature, combined with the presence of a small trioctahedral component in the margarite, suggests that substitutions of the type $^{IV}Al_3{}^{VI}(Fe^{3+},Al)Si_{-3}{}^{VI}\square_{-1}$ and $Na_3{}^{VI}(Fe^{3+},Al)Ca_{-3}{}^{VI}\square_{-1}$ may operate in Ca–Na micas. Margarite (and paragonite) display considerably less octahedral substitution of iron than the associated muscovite. A characteristic feature of margarite is the complete occupancy of its interlayer, in contrast with paragonite and especially muscovite, where the interlayer is usually not fully occupied.

(3) The Si-undersaturated composition of the metabauxites generally inhibits extensive Tschermak substitution $(Si < 6.32$ atoms p.f.u.) in the muscovite, whereas the Fe-rich and oxidized nature of the rocks promotes $^{VI}(Fe^{3+}Al_{-1})$ substitution. As muscovite generally coexists with haematite–ilmenite solid solutions and/or magnetite, most iron in muscovite (and other micas) is probably ferric. Muscovite in the greenschist-grade zones displays combined Tschermak and $^{VI}(Fe^{3+}Al_{-1})$ substitution, whereas $^{VI}(Fe^{3+}Al_{-1})$ substitution predominates in the muscovite of the amphibolite-grade zones.

(4) Muscovite formed during the M_1 (high-P) event largely failed to recrystallize and equilibrate at the greenschist grade of the M_2 event, as indicated by microstructural observations, the results of Ms–Pg solvus thermometry and irregular Na partitioning between muscovite and margarite. The occurrence of relict M_1 muscovite up to staurolite-grade conditions (particularly in commercial emery and kyanitites) implies that K-micas respond sluggishly to changing $P–T$ conditions, as documented in many other studies.

(5) The measured Ca–Na–K partitioning among the white micas documents that primary margarite has a higher $Na/(Na + K + Ca)$ ratio than coexisting muscovite. The metabauxitic plagioclase, forming at the expense of margarite at amphibolite grade, is usually more calcic than margarite, in contrast to observations in quartz-bearing (marly) rocks, where margarite is the more calcic phase. This reversal in Ca–Na partitioning may be a result of the Al-excess (Si-deficient) rock composition and the high metamorphic grade required to stabilize the assemblage margarite–plagioclase–corundum. It could also relate to compositional gaps in calcic plagioclase.

(6) Naturally coexisting Ca–Na mica pairs from this and other studies show considerably less mutual solubility than suggested by the experimental study of the Mrg–Pg join (Franz et al., 1977). The irregular Na distribution between margarite and muscovite as observed in metamorphic rocks may relate to opposing effects of pressure on the Mrg–Pg and Ms–Pg solvi.

ACKNOWLEDGEMENTS

REFERENCES

Ackermand, D. & Morteani, G., 1973. Occurrences and break-down of paragonite and margarite in the Greiner Schiefer Series (Zillerthal Alps, Tyrol). *Contributions to Mineralogy and Petrology* **40**, 293–304.

Ahn, J. H., Peacor, D. R. & Essene, E. J., 1985. Coexisting paragonite–phengite in blueschist eclogite: a TEM study. *American Mineralogist* **70**, 1193–1204.

Andreasson, P. G. & Lagerblad, B., 1980. Occurrence and significance of inverted metamorphic gradients in the western Scandinavian Caledonides. *Journal of the Geological Society London* **137**, 219–230.

Andriessen, P. A. M., 1978. Isotopic age relations within the polymetamorphic complex of the island of Naxos (Cyclades, Greece). Ph.D. Thesis, University of Amsterdam. *Verhandelingen ZWO-Laboratorium voor Isotopen Geologie* **3**, 71 pp.

Andriessen, P. A. M., Boelrijk, N. A. I. M., Hebeda, E. H., Priem, H. N., Verdurmen, E. A. Th. & Verschure, R. H., 1979. Dating the events of metamorphism and granitic magmatism in the Alpine orogen of Naxos (Cyclades, Greece). *Contributions to Mineralogy and Petrology* **69**, 215–225.

Andriessen, P. A. M., Banga, G. & Hebeda, E. H., 1987. Isotopic age study of pre-Alpine rocks in the basal units on Naxos, Sikinos and Ios, Greek Cyclades. *Geologie en Mijnbouw* **66**, 3–14.

Baker, J. & Matthews, A., 1994. Textural and isotopic development of marble assemblages during the Barrovian-style M_2 metamorphic event, Naxos, Greece. *Contributions to Mineralogy and Petrology* **116**, 130–144.

Baltatzis, E. & Katagas, C., 1981. Margarite pseudomorphs after kyanite in Glen Esk, Scotland. *American Mineralogist* **66**, 213–216.

Bardossy, G., 1982. Karstbauxites: bauxite deposits on carbonate rocks. In: *Developments in Economic Geology 14*. Amsterdam: Elsevier.

Blencoe, J. G., Guidotti, C. V. & Sassi, F. P., 1994. The paragonite–muscovite solvus: II. Numerical geothermometers for natural, quasibinary paragonite–muscovite pairs. *Geochimica et Cosmochimica Acta* **58**, 2277–2288.

Bröcker, M., Kreuzer, H., Matthews, A. & Okrusch, M., 1993. $^{40}Ar/^{39}Ar$ and oxygen isotope studies of polymetamorphism from Tinos island, Cycladic blueschist belt, Greece. *Journal of Metamorphic Geology* **11**, 223–240.

Bucher, K. & Frey, M., 1994. *Petrogenesis of Metamorphic Rocks*, 6th edn. Berlin: Springer-Verlag.

Bucher, K., Frank, E. & Frey, M., 1983. A model for the progressive regional metamorphism of margarite-bearing rocks in the central Alps. *American Journal of Science* **283-A**, 370–395.

Buick, I. S., 1991. The late Alpine evolution of an extensional shear zone, Naxos, Greece. *Journal of the Geological Society London* **148**, 93–103.

Buick, I. S. & Holland, T. J. B., 1989. The *P–T–t* path associated with crustal extension, Naxos, Cyclades, Greece. In: Daly, J. S., Cliff, R. A. & Yardley, B. W. D. (eds) Evolution of Metamorphic Belts. *Special Publication, Geological Society of London* **43**, 365–369.

Buick, I. S. & Holland, T. J. B., 1991. The nature and distribution of fluids during amphibolite facies metamorphism, Naxos (Greece). *Journal of Metamorphic Geology* **9**, 301–314.

Carpenter, M. A., 1988. Thermochemistry of aluminium/silicon ordering in feldspar minerals. In: Salje, E. K. H. (ed.) *Physical Properties and Thermodynamic Behaviour of Minerals. NATO ASI Series C 225.* Dordrecht: D. Reidel, pp. 265–323.

Chatterjee, N. D., 1974. Synthesis and upper thermal stability limit of 2M-margarite $CaAl_2[Al_2Si_2O_{10}/(OH)_2]$. *Schweizerische mineralogische und petrographische Mitteilungen* **54**, 753–767.

Chatterjee, N. D. & Flux, S., 1986. Thermodynamic mixing properties of muscovite–paragonite crystalline solutions at high temperatures and pressures, and their geological applications. *Journal of Petrology* **27**, 677–693.

Chatterjee, N. D. & Froese, E., 1975. A thermodynamic study of the pseudobinary join muscovite–paragonite in the system $KAlSi_3O_8–NaAlSi_3O_8–Al_2O_3–SiO_2–H_2O$. *American Mineralogist* **60**, 985–993.

Chatterjee, N. D. & Warhus, U., 1984. Ephesite, $Na(LiAl_2)[Al_2Si_2O_{10}](OH)_2$: II. Thermodynamic analysis of its stability and compatibility relations, and its geological occurrences. *Contributions to Mineralogy and Petrology* **85**, 80–84.

Chopin, C. & Maluski, H., 1980. $^{40}Ar–^{39}Ar$ dating of high pressure metamorphic micas from the Gran Paradiso Area (Western Alps): evidence against the blocking temperature concept. *Contributions to Mineralogy and Petrology* **74**, 109–122.

Cliff, G. A. & Lorimer, G. W., 1975. The quantitative analysis of thin specimens. *Journal of Microscopy* **103**, 203–207.

Cooper, A. F., 1980. Retrograde alteration of chromian kyanite in metachert and amphibolite whiteschist from the Southern Alps, New Zealand, with implications for uplift on the Alpine Fault. *Contributions to Mineralogy and Petrology* **75**, 153–164.

Dempster, T. J., 1992. Zoning and recrystallization of phengitic micas: implications for metamorphic equilibration. *Contributions to Mineralogy and Petrology* **109**, 526–537.

Dixon, J. E., Feenstra, A., Jansen, J. B. H., Kreulen, R., Ridley, J., Salemink, J. & Schuiling, R. D., 1987. Excursion guide to the field trip on Seriphos, Syros and Naxos. In: Helgeson, H. C. (ed.) *Chemical Transport in Metasomatic Processes. NATO ASI Series C 218.* Dordrecht: D. Reidel, pp. 467–518.

Dürr, St., 1986. Das Attisch–Kykladische Kristallin. In: Jacobshagen, V. (ed.) *Geologie von Griechenland*. Berlin: Gebrüder Bornträger, pp. 116–149.

Dyar, M. D., Guidotti, C. V., Holdaway, M. J. & Colucci, M., 1993. Nonstoichiometric hydrogen contents in common rock-forming hydroxyl silicates. *Geochimica et Cosmochimica Acta* **57**, 2913–2918.

Enami, M., 1980. Notes on petrography and rock-forming mineralogy (8) Margarite-bearing metagabbro from the Iratsu mass in the Sanbagawa Belt, Central Shikoku. *Journal Japanese Association Mineralogy Petrology Economic Geology* **75**, 245–253.

Essene, E. J., 1989. The current status of thermobarometry in metamorphic rocks. In: Daly, J. S., Cliff, R. A. & Yardley, B. W. D. (eds) *Evolution of Metamorphic Belts. Special Publication, Geological Society of London* **43**, 1–44.

Eugster, H. P., Albee, A. L., Bence, A. E., Thompson, J. B., Jr & Waldbaum, D. R., 1972. The two-phase region and excess mixing properties of paragonite–muscovite crystalline solutions. *Journal of Petrology* **13**, 147–179.

Feenstra, A., 1985. Metamorphism of bauxites on Naxos, Greece. Ph.D. Thesis, University of Utrecht. *Geologica Ultraiectina* **39**, 206 pp.

Feenstra, A. & Maksimovic, Z., 1985. Geochemistry of diaspore and corundum-bearing metabauxites from Naxos, Greece. Part 1: major and trace element chemistry, and geochemical evidence of a Jurassic stratigraphic age. In: Feenstra, A.: Metamorphism of bauxites on Naxos, Greece. Ph.D. Thesis, University of Utrecht. *Geologica Ultraiectina* **39**, 137–173.

Frank, E., 1983. Alpine metamorphism of calcareous rocks along a cross-section in the Central Alps: occurrence and breakdown of

muscovite, margarite and paragonite. *Schweizerische mineralogische und petrographische Mitteilungen* 63, 37–93.

Franz, G., Hinrichsen, T. & Wannemacher, E., 1977. Determination of the miscibility gap on the solid solution series paragonite–margarite by means of infrared spectroscopy. *Contributions to Mineralogy and Petrology* 59, 307–316.

Frey, M., 1978. Progressive low-grade metamorphism of a black shale formation, Central Swiss Alps, with special reference to pyrophyllite and margarite bearing assemblages. *Journal of Petrology* 19, 95–135.

Frey, M., 1987. Very low-grade metamorphism of clastic sedimentary rocks. In: Frey, M. (ed.) *Low Temperature Metamorphism*. Glasgow: Blackie, pp. 9–58.

Frey, M. & Orville, P. M., 1974. Plagioclase in margarite-bearing rocks. *American Journal of Science* 274, 31–47.

Frey, M., Bucher, K., Frank, E. & Schwander, H., 1982. Margarite in the Central Alps. *Schweizerische mineralogische und petrographische Mitteilungen* 62, 21–45.

Frey, M., Hunziker, J. C., Jäger, E. & Stern, W. B., 1983. Regional distribution of white K-mica polymorphs and their phengite content in the Central Alps. *Contributions to Mineralogy and Petrology* 83, 185–197.

Gal, L. P. & Ghent, E. D., 1991. Margarite-bearing pelites from the Western Rocky Mountains, northwest of Golden, British Columbia. *Canadian Mineralogist* 29, 11–19.

Gibson, G. M., 1979. Margarite in kyanite- and corundum-bearing anorthosite, amphibolite, and hornblendite from Central Fiordland, New Zealand. *Contributions to Mineralogy and Petrology* 68, 171–179.

Grew, E. S., Hinthorne, J. R. & Marquez, N., 1986. Li, Be, B and Sr in margarite and paragonite from Antarctica. *American Mineralogist* 71, 1129–1134.

Grove, T. L., Ferry, J. M. & Spear, F. S., 1983. Phase transitions and decomposition relations in calcic plagioclase. *American Mineralogist* 68, 41–59.

Guggenheim, S. & Bailey, S. W., 1978. Refinement of the margarite structure in subgroup symmetry: correction, further refinement, and comments. *American Mineralogist* 63, 186–187.

Guidotti, C. V., 1984. Micas in metamorphic rocks. In: Bailey, S. W. (ed.) *Micas. Mineralogical Society of America, Reviews in Mineralogy* 13, 357–467.

Guidotti, C. V. & Cheney, J. T., 1976. Margarite pseudomorphs after chiastolite in the Rangeley area, Maine. *American Mineralogist* 61, 431–434.

Guidotti, C. V. & Dyar, M. D., 1991. Ferric iron in metamorphic biotite and its petrologic and crystallochemical implications. *American Mineralogist* 76, 161–175.

Guidotti, C. V., Post, J. L. & Cheney, J. T., 1979. Margarite pseudomorphs after chiastolite in the Georgetown area, California. *American Mineralogist* 64, 728–732.

Guidotti, C. V., Sassi, F. P., Blencoe, J. G. & Selverstone, J., 1994a. The paragonite–muscovite solvus: I. *P–T–X* limits derived from the Na–K compositions of natural, quasibinary paragonite–muscovite pairs. *Geochimica et Cosmochimica Acta* 58, 2269–2275.

Guidotti, C. V., Sassi, F. P., Sassi, R. & Blencoe, J. G., 1994b. The effects of ferromagnesian components on the paragonite–muscovite solvus: a semiquantitative analysis based on chemical data for natural paragonite–muscovite pairs. *Journal of Metamorphic Geology* 12, 779–788.

Guidotti, C. V., Yates, M. G., Dyar, M. D. & Taylor, M. E., 1994c. Petrogenetic implications of the Fe^{3+} content of muscovite in pelitic schists. *American Mineralogist* 79, 793–795.

Höck, V., 1974. Coexisting phengite, paragonite and margarite in metasediments of the Mittlere Hohe Tauern, Austria. *Contributions to Mineralogy and Petrology* 43, 261–273.

Hoinkes, G., 1978. Zur Mineralchemie und Metamorphose toniger und mergeliger Zwischenlagen in Marmoren des südwestlichen Schneebergerzuges (Ötztaler Alpen, Südtirol). *Neues Jahrbuch für Mineralogie, Abhandlungen* 131, 272–303.

Jacobshagen, V., 1994. Orogenic evolution of the Hellenides: new aspects. *Geologische Rundschau* 83, 249–256.

Jansen, J. B. H., 1977. Metamorphism on Naxos. Ph.D. Thesis, University of Utrecht.

Jansen, J. B. H. & Schuiling, R. D., 1976. Metamorphism on Naxos: petrology and geothermal gradients. *American Journal of Science* 276, 1225–1253.

Jiang, W-T. & Peacor, D. R., 1993. Formation and modification of metastable intermediate sodium potassium mica, paragonite, and muscovite in hydrothermally altered metabasites from northern Wales. *American Mineralogist* 78, 782–793.

Joswig, W., Takéuchi, Y. & Fuess, H., 1983. Neutron-diffraction study on the orientation of hydroxyl groups in margarite. *Zeitschrift für Kristallographie* 165, 295–303.

Kretz, R., 1983. Symbols for rock-forming minerals. *American Mineralogist* 68, 277–279.

Langer, K., Chatterjee, N. D. & Abraham, K., 1981. Infrared studies of some synthetic and natural $2M_1$ dioctahedral micas. *Neues Jahrbuch für Mineralogie, Abhandlungen* 142, 91–110.

Lin, C. & Bailey, S. W., 1984. The crystal structure of paragonite-$2M_1$. *American Mineralogist* 69, 122–127.

Lister, G. S., Banga, G. & Feenstra, A., 1984. Metamorphic core complexes of Cordilleran type in the Cyclades, Aegean Sea, Greece. *Geology* 12, 221–225.

Lorimer, G. W., 1987. Quantitative X-ray microanalysis of thin specimens in the transmission electron microscope; a review. *Mineralogical Magazine* 51, 49–60.

Loucks, R. R., 1991. The bound interlayer H$_2$O content of potassic white micas: muscovite–hydromuscovite–hydropyrophyllite solutions. *American Mineralogist* 76, 1563–1579.

Massone, H-J. & Schreyer, W., 1987. Phengite geobarometry based on the limiting assemblage with K-feldspar, phlogopite and quartz. *Contributions to Mineralogy and Petrology* 96, 212–224.

Meyer, J., 1983. Mineralogie und Petrologie des Allalingabbros. Ph.D. Thesis, University of Basel, 331 pp.

Morand, V. J., 1988. Vanadium-bearing margarite from the Lachlan Fold Belt, New South Wales, Australia. *Mineralogical Magazine* 52, 341–345.

Okrusch, M. & Bröcker, M., 1990. Eclogites associated with high-grade blueschists in the Cyclades archipelago, Greece: a review. *European Journal of Mineralogy* 2, 451–478.

Okuyama-Kusunose, Y., 1985. Margarite–paragonite–muscovite assemblages from the low-grade metapelites of the Tono metamorphic aureole, Kitakama Mountains, Northeast Japan. *Journal Japanese Association Mineralogy Petrology Economic Geology* 80, 515–525.

Petrakakis, K. & Jawecki, C., 1995. Metamorphism and retrogression of Moldanubian granulites. *European Journal of Mineralogy* 7, 1183–1203.

Robertson, A. H. F. & Dixon, J. E., 1984. Introduction: aspects of the geological evolution of the Eastern Mediterranean. In: Dixon, J. E. & Robertson, A. H. F. (eds) *The Geological Evolution of the Eastern Mediterranean. Special Publication, Geological Society of London* 17, 1–74.

Sagon, J.-P., 1967. Le métamorphisme dans le Nord-Est du bassin de Châteaulin: découverte de chloritoïde et de margarite dans

les schistes dévoniens. *Comptes Rendus Sommaires des Séances de la Société Géologique de France* 5, 206–207.

Scaillet, S., Feraud, G., Ballevre, M. & Amouric, M., 1992. Mg/Fe and [(Mg,Fe)Si-Al$_2$] compositional control on argon behaviour in high-pressure white micas: a ^{40}Ar/^{39}Ar continuous laser-probe study from the Dora–Maira nappe of the internal Alps, Italy. *Geochimica et Cosmochimica Acta* 56, 2851–2872.

Schaller, W. T., Carron, M. K. & Fleischer, M., 1967. Ephesite, Na(LiAl$_2$)(Al$_2$Si$_2$)O$_{10}$(OH)$_2$, a tri-octahedral member of the margarite group, and related brittle micas. *American Mineralogist* 52, 1689–1696.

Schliestedt, M., 1986. Eclogite–blueschist relationships as evidenced by mineral equilibria in the high-pressure rocks of Sifnos (Cycladic islands), Greece. *Journal of Petrology* 27, 1437–1459.

Schliestedt, M., Altherr, R. & Matthews, A., 1987. Evolution of the Cycladic Crystalline Complex: petrology, isotope geochemistry and geochronology. In: Helgeson, H. C. (ed.) *Chemical Transport in Metasomatic Processes. NATO ASI Series C 218.* Dordrecht: D. Reidel, pp. 389–428.

Shau, Y-H., Feather, M. E., Essene, E. J. & Peacor, D. R., 1991. Genesis and solvus relations of submicroscopically intergrown paragonite and phengite in a blueschist from northern California. *Contributions to Mineralogy and Petrology* 106, 367–378.

Smith, D. C. & Kechid, S. A., 1983. Three rare Al- and Na-rich micas in the Liset eclogite pod, Norway: Mg–Fe-margarite, preiswerkite and Na-eastonite. *Terra Cognita* 3, 191.

Smith, J. L., 1850. Memoir on emery—First part—On the geology and mineralogy of emery from observations made in Asia Minor. *American Journal of Science* 10, 354–369.

Smith, J. L., 1851. Mineral-Substanzen, den Schmirgel in Kleinasien begleitend. *Neues Jahrbuch für Mineralogie, Geognosie, Geologie,* Jahrgang 1851, 589–590.

Smith, J. V., 1983. Phase equilibria of plagioclase. In: Ribbe, P. H. (ed.) *Feldspar Mineralogy. Mineralogical Society of America, Reviews in Mineralogy* 2, 223–239.

Stähle, V., Frenzel, G. & Mertz, D. F., 1986. Retrograde metamorphism in anorthositic layers from Finero (Ivrea zone). *Schweizerische mineralogische und petrographische Mitteilungen* 66, 73–98.

Stöckert, B., 1985. Compositional control on the polymorphism (2M$_1$–3T) of phengitic white mica from high pressure parageneses of the Sesia Zone (lower Aosta valley, Western Alps; Italy). *Contributions to Mineralogy and Petrology* 89, 52–58.

Teale, G. S., 1979. Margarite from the Olary Province of South Australia. *Mineralogical Magazine* 43, 433–435.

Thompson, A. B., Lyttle, P. T. & Thompson, J. B., Jr, 1977. Mineral reactions and A–Na–K and A–F–M facies types in the Gassetts schist, Vermont. *American Journal of Science* 277, 1124–1151.

Urai, J. L., Schuiling, R. D. & Jansen, J. B. H., 1990. Alpine deformation on Naxos (Greece). In: Knipe, R. J. & Rutter, E. H. (eds) *Deformation Mechanisms, Rheology and Tectonics. Special Publication, Geological Society of London* 54, 509–522.

Vance, D. & Holland, T., 1993. A detailed isotopic and petrological study of a single garnet from the Gassetts schist, Vermont. *Contributions to Mineralogy and Petrology* 114, 101–118.

Van der Maar, P. A., 1981. Metamorphism on Ios and the geological history of the southern Cyclades, Greece. Ph.D. Thesis, University of Utrecht. *Geologica Ultraiectina* 28, 142 pp.

Van der Maar, P. A. & Jansen, J. B. H., 1983. The geology of the polymetamorphic complex of Ios, Cyclades, Greece, and its significance for the Cycladic Massif. *Geologische Rundschau* 72, 283–299.

Van der Maar, P. A., Feenstra, A., Manders, B. & Jansen, J. B. H., 1981. The petrology of the island of Sikinos, Cyclades, Greece, in comparison with that of the adjacent island of Ios. *Neues Jahrbuch für Mineralogie Monatshefte,* Jahrgang 1981, 459–469.

Veblen, D. R. & Ferry, J. M., 1983. A TEM study of the biotite–chlorite reaction and comparison with petrologic observations. *American Mineralogist* 68, 1160–1169.

Voncken, J. H. L., van der Eerden, A. M. J. & Jansen, J. B. H., 1987a. Synthesis of a Rb analogue of 2M$_1$ muscovite. *American Mineralogist* 72, 551–554.

Voncken, J. H. L., Wevers, J. M. A. R., van der Eerden, A. M. J., Bos, A. & Jansen, J. B. H., 1987b. Hydrothermal synthesis of tobelite, NH$_4$Al$_2$Si$_3$AlO$_{10}$(OH)$_2$, from various starting materials and implications for its occurrence in nature. *Geologie en Mijnbouw* 66, 259–269.

Wenk, E., Schwander, H. & Wenk, H.-R., 1991. Microprobe analyses of plagioclases from metamorphic carbonate rocks of the Central Alps. *European Journal of Mineralogy* 3, 181–191.

Williams, M. L. & Grambling, J., A., 1990. Manganese, ferric iron, and the equilibrium between garnet and biotite. *American Mineralogist* 75, 886–908.

Wybrans, J. R. & McDougall, I., 1986. ^{40}Ar/^{39}Ar dating of white micas from an Alpine high-pressure metamorphic belt on Naxos (Greece): the resetting of the argon isotopic system. *Contributions to Mineralogy and Petrology* 93, 187–194.

Wybrans, J. R. & McDougall, I., 1988. Metamorphic evolution of the Attic Cycladic Metamorphic Belt on Naxos (Cyclades, Greece) utilizing ^{40}Ar/^{39}Ar age spectrum measurements. *Journal of Metamorphic Geology* 6, 571–594.

Yalçin, U., Schreyer, W. & Medenbach, O., 1993. Zn-rich högbomite formed from gahnite in the metabauxites of the Menderes Massif, SW Turkey. *Contributions to Mineralogy and Petrology* 113, 314–324.

Yardley, B. W. D. & Baltatzis, E., 1985. Retrogression of staurolite schists and the sources of infiltrating fluids during metamorphism. *Contributions to Mineralogy and Petrology* 89, 59–68.

Appendix: Compositional data for coexisting margarite, muscovite, paragonite and plagioclase plotted in Figs 13 and 14

Sample no.	Zone	Margarite					Muscovite						Paragonite			
		XCa	XNa	XK	Fe+Mg	No. an.	XCa	XNa	XK	Si	Fe+Mg	No. an.	XCa	XNa	XK	Fe+Mg
THIS STUDY																
Greenschist grade																
IO-76-2	Ios	0·719	0·252	0·029	0·05	4	0·000	0·119	0·881	6·16	0·33	4	n.a.			
IO-76-2	Ios	0·663	0·306	0·031	0·05	4	0·000	0·132	0·868	6·13	0·39	3	n.a.			
135C	II	0·838	0·145	0·017	0·06	4	0·000	0·122	0·878	6·18	0·30	5				
135D	II	0·881	0·098	0·021	0·05	5	0·000	0·103	0·897	6·16	0·31	12				
156A	II	0·868	0·108	0·024	0·05	13	0·002	0·089	0·909	6·16	0·31	11				
133A	II	0·686	0·290	0·025	0·07	19	0·000	0·144	0·856	6·15	0·31	32	n.a.			
133A	II	0·651	0·340	0·009	0·08	4	0·000	0·164	0·836	6·11	0·39	3	n.a.			
03C3	III	0·742	0·247	0·011	0·16	5	0·000	0·124	0·876	6·15	0·35	4	n.a.			
03C3	III	0·649	0·324	0·027	0·13	2	0·000	0·153	0·847	6·13	0·33	3	n.a.			
22B	III	0·847	0·114	0·040	0·09	8	0·011	0·083	0·906	6·20	0·27	7				
B610-5	III	0·663	0·306	0·031	0·12	7	0·000	0·177	0·823	6·18	0·40	15	0·033	0·876	0·091	0·09*
AF23-2	III	0·668	0·310	0·022	0·08	2	0·000	0·153	0·847	6·22	0·36	9	n.a.			

Sample no.	Zone	Margarite					Muscovite						Plagioclase			
		XCa	XNa	XK	Fe+Mg	No. an.	XCa	XNa	XK	Si	Fe+Mg	No. an.	XCa	XNa	XK	No. an.
Amphibolite grade																
128A	IVI	0·881	0·112	0·008	0·14	14	0·000	0·063	0·937	6·14	0·20	3	0·938	0·057	0·005	7
105B	IVm	0·896	0·080	0·024	0·08	3	0·000	0·035	0·965	6·21	0·37	6				
116E	IVm	0·870	0·117	0·013	0·07	3	0·000	0·038	0·962	6·13	0·37	5				
106-2	IVm	0·849	0·133	0·018	0·06	6	0·000	0·067	0·933	6·13	0·41	5	0·952	0·042	0·006	7
24K4A	IVm	0·697	0·273	0·029	0·09	4	0·000	0·105	0·895	6·08	0·37	3	0·878	0·122	0·000	4
24L	IVm	0·697	0·261	0·041	0·07	5	0·000	0·073	0·927	6·13	0·41	14	0·895	0·098	0·007	10
104B	IVu	0·674	0·317	0·010	0·10	8	0·000	0·130	0·870	6·05	0·46	8	0·406	0·594	0·000	8
104BN42	IVu	0·746	0·205	0·049	0·10	5	0·000	0·093	0·907	6·02	0·34	6				

Retrograde

															Paragonite			
B492B	IVl	0·743	0·245	0·012	0·13	13	0·000	0·204	0·796	6·05	0·20	11						
113-4	IVm	0·960	0·040	0·000	0·06	9	0·000	0·035	0·965	6·06	0·38	6						
150B	IVm	0·949	0·047	0·004	0·06	5	0·000	0·063	0·937	6·12	0·33	12	0·953	0·042	0·005	9		
116F	IVm	0·873	0·113	0·014	0·09	4	0·000	0·122	0·878	6·14	0·41	10						

LITERATURE DATA

Locality	Ref													XCa	XNa	XK	Fe + Mg
Greenschist grade																	
Hohe Tauern, Austria	1	0·691	0·294	0·015	0·02		0·000	0·094	0·906	6·37	0·40		0·020	0·904	0·076	0·06
Kitakami Mts, Japan	2	0·799	0·192	0·010	0·05		0·010	0·137	0·854	6·20	0·20		0·043	0·908	0·049	0·04
Amphibolite grade																	
Zillerthal, Austria	3	0·628	0·343	0·029	0·14								0·045	0·875	0·080	0·06
Dalradian, Scotland	4	0·679	0·302	0·019	0·12	16	0·008	0·210	0·785	6·24	0·35	16	0·083	0·828	0·088	0·07†
Retrograde																	
Sanbagawa Belt, Japan	5	0·757	0·242	0·002	0·13								0·045	0·912	0·044	0·02
Antarctica	6	0·783	0·215	0·003	0·18								0·073	0·874	0·054	0·08
Georgetown area, USA	7	0·791	0·209	0·001	0·05		0·004	0·210	0·786	6·18	0·14		0·106	0·770	0·125	0·09

XCa, mole fraction Ca/(Ca + Na + K); XNa, mole fraction Na/(Ca + Na + K); XK, mole fraction K/(Ca + Na + K). (Fe + Mg) and Si are given as atoms per 22 oxygens assuming all Fe is ferric in the metabauxitic micas and all Fe is ferrous in the other micas. No. an., number of EMP analyses on which averages are based. n.a., present but not analysed. *Average is based on eight analyses. †Average is based on 19 analyses.

References: (1) Höck (1974, sample 131/70); (2) Okuyama-Kusunose (1985, average of samples 14.01 and 09.05); (3) Ackermand & Morteani (1973, average of samples 70.63, 70.64, 828 and Gr.ST1); (4) Lorimer [1987, sample DAL43 of A. Feenstra & P. E. Champness (unpublished)]; (5) Enami (1980); (6) Grew *et al.* (1986, sample 4017E); (7) Guidotti *et al.* (1979, average of samples P-1 and P-2).